Ricardo Rodrigues Justino da Silva

Critical Phenomena in *Rock-Paper-Scissors* Model

São Carlos - SP, Brazil

May, 2024

Ricardo Rodrigues Justino da Silva

Critical Phenomena in *Rock-Paper-Scissors* Model

Tese apresentada ao Programa de Pós-Graduação em Física da Universidade Federal de São Carlos como parte dos requisitos exigidos para a obtenção do título de Doutor em Ciências.
Área de Concentração: Física Básica.

Universidade Federal de São Carlos

Centro de Ciências Exatas e de Tecnologia

Programa de Pós-Graduação em Física

Supervisor: Prof. Dr. Francisco Ednilson Alves dos Santos

São Carlos - SP, Brazil

May, 2024

UNIVERSIDADE FEDERAL DE SÃO CARLOS

Centro de Ciências Exatas e de Tecnologia
Programa de Pós-Graduação em Física

Folha de Aprovação

Defesa de Tese de Doutorado do candidato Ricardo Rodrigues Justino da Silva, realizada em 07/05/2024.

Comissão Julgadora:

Prof. Dr. Francisco Ednilson Alves dos Santos (UFSCar)

Prof. Dr. Paulo Cesar de Camargo (UFSCar)

Prof. Dr. Renan da Silva Souza (Goethe-Universität)

Prof. Dr. Cláudio Lucas Nunes de Oliveira (UFC)

Prof. Dr. Dionísio Bazeia Filho (UFPB)

O Relatório de Defesa assinado pelos membros da Comissão Julgadora encontra-se arquivado junto ao Programa de Pós-Graduação em Física.

In memoriam tio Carlos.

Agradecimentos

Expresso minha profunda gratidão e admiração ao Professor Dr. Francisco Ednilson por sua orientação perspicaz, paciência e apoio inestimável. Em momentos em que nem eu acreditava em meu próprio potencial, o senhor mostrou confiança em minhas capacidades. Com sua experiência e paciência, me inspirou a superar as expectativas e concluir este trabalho.

Agradeço sinceramente ao Professor Dr. Dionio Bazeia por sua valiosa colaboração e contribuições enriquecedoras ao presente trabalho.

Ao meu grande amigo Marcos Alberto, cuja paciência e ajuda foram imprescindíveis para a realização do presente trabalho. As incontáveis horas de conversa e trocas de mensagens foram fundamentais. Obrigado Marcão, você é o BRABO!

Expresso minha gratidão ao Professor Dr. Leonardo Castelano, que não apenas foi meu primeiro professor de física computacional, mas também inspirou meu interesse pelo assunto.

Expresso minha profunda gratidão aos meus pais, Cícero Justino e Rita de Cássia, pelo seu amor sereno e apoio constante. Mesmo sem compreender plenamente o foco do meu trabalho e enfrentando recursos limitados, vocês investiram tudo o que foi necessário para que eu continuasse a perseguir meus sonhos. Jamais esquecerei o dia em que, após enfrentar dificuldades significativas, precisei sair de São Carlos. Naquele momento difícil, vocês me acolheram e me deram forças para retornar e reorganizar minha trajetória. Gratidão eterna!

Ao meu grande amor e companheira, Maju, que esteve ao meu lado nos momentos mais desafiadores e turbulentos. Com sua paciência e perseverança, você me ajudou a levantar e seguir em frente, ensinando-me que a vida pode ser vivida de maneira leve. Minha profunda gratidão a você e sua família por me receberem com tanto carinho em terras Sancarlinas.

Aos meus P.R.I.M.O.S, agradeço pelo verdadeiro companheirismo e pelas inúmeras aventuras. Juntos, compartilhamos cervejas, brindes e churrascos, momentos preciosos para celebrar a vida, desabafar e planejar o futuro. Independentemente da distância, a essência de nossa amizade pura sempre permaneceu forte.

Agradeço imensamente aos meus irmãos, Bruno e Maria de Fátima, assim como a toda minha família e amigos, pelo apoio constante e inabalável. Sua presença e encorajamento têm sido fundamentais em minha jornada.

À minha prima Jacke, minha gratidão por sua paciência ao esclarecer minhas

dúvidas de matemática durante o primário. Sua ajuda foi crucial para minha jornada acadêmica e esta conquista.

Ao meu tio e padrinho Josa, que, embora talvez ainda não compreenda completamente minha decisão de migrar para o interior de São Paulo em busca de melhores oportunidades, sempre me ofereceu seu apoio constante, inclusive durante minhas aventuras internacionais.

À galerinha da AFEF — atletas, amigos e membros — que estiveram comigo durante o meu período de gestão, agradeço profundamente. Os momentos de descontração e amizade no esporte foram essenciais e enriquecedores nesta fase da minha vida.

Aos amigos e à família TIF, vocês têm um lugar especial no meu coração. Continuarei apoiando e incentivando nossas iniciativas de enriquecer a vida dos estudantes através do esporte e da construção de amizades duradouras.

À minha querida professora do ensino fundamental, Neusa Maria, agradeço por todos aqueles "recreios" em que fiquei de castigo até dominar os conceitos de raiz quadrada e a exponenciação. Essas lições não apenas me ensinaram matemática, mas também o valor inestimável da disciplina e dedicação.

Devo um agradecimento especial a mim mesmo pela dedicação e comprometimento, gerenciando não apenas os complexos planos de ação que tracei ao longo da minha vida, mas também os recursos para torná-los realidade. Os meus "Eus" do passado acreditaram que era possível e, por isso, pavimentaram toda a estrada até aqui. Tenho apenas gratidão pela disciplina que mantive. E, sim, como bem disse Euclides da Cunha, "O sertanejo é, antes de tudo, um forte".

E a todos que, direta ou indiretamente, contribuíram para esta conquista, mesmo aqueles cujos nomes não mencionei aqui, saibam que guardo cada história no coração. Um forte abraço a cada um de vocês.

O presente trabalho foi parcialmente realizado com apoio do Conselho Nacional de Desenvolvimento Científico e Tecnológico (CNPq), utilizando recursos do projeto INTC - MCTI/CNPq/CAPES/FAPs nº 16/2014.

"O sertanejo é, antes de tudo, um forte . . . "

Euclydes da Cunha, Os Sertões.

Resumo

Este trabalho apresenta um estudo da dinâmica do modelo Pedra-Papel-Tesoura (RPS), com particular ênfase na influência das variações dos parâmetros de controle na emergência e dissipação de padrões espaciais à medida que o sistema se aproxima de um valor crítico. Observamos que o modelo exibe transição de fase contínua, da fase simétrica para a não simétrica. Utilizamos como ferramenta de análise, o referencial teórico dos fenômenos críticos para explorar a estabilidade do sistema, na região próxima do ponto crítico, com isso foi possível realizar o cálculo dos expoentes críticos. Esta pesquisa é importante para uma melhor compreensão dos intrincados comportamentos e padrões observados neste tipo de sistema, contribuindo significativamente para o campo geral da pesquisa de sistemas complexos. Além disso, este trabalho estabelece uma ligação importante entre a teoria dos fenômenos críticos e a dinâmica do modelo RPS, centrando-se na emergência do comportamento crítico e nas condições que conduzem à criticalidade e na possível caracterização da classe de universalidade. Em suma, embora tenha sido viável calcular os expoentes críticos do modelo Rock-Paper-Scissors (RPS), a identificação específica da sua classe de universalidade permanece indefinida. Esta limitação decorre da prioridade dada neste trabalho ao desenvolvimento de novos métodos capazes de extrair informações significativas sobre o comportamento crítico de sistemas não diretamente relacionados à termodinâmica. Ainda assim, a obtenção dos expoentes críticos é uma conquista notável, ressaltando o potencial inexplorado do modelo RPS. Este modelo se apresenta como uma forma promissora de abordar sistemas complexos, tanto no âmbito da física quanto da biologia, sugerindo um vasto campo de possibilidades para futuras investigações e aplicações.

Palavras-chave: Fenômenos Críticos. Expoentes Críticos. Modelo Rock-Paper-Scissors. Biodiversidade. Formação de Padrões. Dinâmica de Populações.

Abstract

This work presents a study on the dynamics of the Rock-Paper-Scissors (RPS) model, with particular emphasis on the influence of variations of the control parameters on the emergence and dissipation of spatial patterns as the system approaches a critical value. We observed that the model exhibits a continuous phase transition from the symmetric to the non-symmetric phase. We used the theoretical framework of critical phenomena as an analytical tool to explore the system stability in the vicinity of the critical point, allowing the calculation of the critical exponents. This research is important for a better understanding of the intricate behaviors and patterns observed in this type of system, and contributes significantly to the general field of complex systems research. Furthermore, this work established a link between the theory of critical phenomena and the dynamics of the RPS model, focusing on the emergence of critical behavior and the conditions that led to criticality and the characterization of the universality class. In summary, although it has been possible to obtain the critical exponents of the Rock-Paper-Scissors (RPS) model, the specific identification of its universality class remains unclear. This limitation results from the priority given in this thesis to the development of advanced methods capable of extracting significant information from the critical behavior of systems not directly related to thermodynamics. Nevertheless, obtaining the critical exponents is already an interesting achievement that emphasizes the unexplored potential of the RPS model. This model presents itself as a promising framework to address more complex questions in physics and biology, suggesting a vast field of possibilities for future investigations and applications.

Keywords: Critical Phenomena. Critical Exponents. Rock-Paper-Scissors Model. Biodiversity. Pattern Formation. Population Dynamics.

List of Figures

List of Tables

List of symbols

μ	Movement
μ_c	Critical Movement
λ	Reproduction
σ	Predation
δ	Critical exponent related to the order parameter
η	Critical exponent related to correlation function decay
γ	Critical exponent related to susceptibility or compressibility
ν	Critical exponent related to correlation length decay
z	Critical exponent related to relaxation time decay
τ	Relaxation time
ρ	Generic control parameter
ξ	Correlation length
$G(\mathbf{r})$	Correlation function in real space
$g(\mathbf{k})$	Correlation function in reciprocal space
l	Species l, where $l = 1, 2, 3$
N	Lattice size
t_i	Generation step
t_N	Total generation
$A^{(l)}$	Abundance of species l
$\langle . \rangle$	Ensemble average
E	Mean square error

Contents

1 Introduction

1.1 Background

The study of critical phenomena and phase transitions has long been a cornerstone of theoretical physics, tracing its roots back to the early 20th century [1, 2]. Initially, the focus was predominantly on equilibrium systems, where phase transitions were understood in terms of changes in thermodynamic variables, such as temperature and pressure. The concept of universality, introduced in the $1960s$ and $70s$, revolutionized the field by revealing that systems with vastly different microscopic properties could exhibit strikingly similar behavior near critical points [1, 2, 3, 4, 5, 6]. This led to the development of the renormalization group theory [4], which provided a deeper understanding of scaling and universality in critical phenomena. Over time, the study of critical phenomena expanded beyond traditional physics, finding applications in a diverse range of fields including chemistry, biology, and even economics [7].

In parallel, the study of stochastic systems, particularly in ecological and social contexts, gained momentum. The Rock-Paper-Scissors (RPS) model emerged as a prominent example, illustrating cyclic dominance and competitive interactions in ecosystems [8, 9]. Initially conceptualized as a simple game theory model, the RPS model has evolved to become a significant tool in understanding biodiversity, species coexistence, and evolutionary dynamics [9]. Its application has extended to various fields, from the study of microbial populations [10] to the analysis of social behaviors [7, 11]. The simplicity of the model, coupled with its ability to capture complex dynamics, makes it an ideal framework for exploring stochastic phenomena [12].

This interdisciplinary approach seeks to apply the principles of scaling, universality, and phase transitions, traditionally associated with equilibrium systems in physics, to the dynamic, stochastic world of ecological and social systems. The potential of this synthesis lies in its ability to provide a deeper understanding of the complex behaviors and patterns observed in these systems [7, 10]. By exploring how the RPS model behaves under different conditions and parameters, we can learn more about the mechanisms that determine biodiversity, stability, and change in ecosystems, contributing to a more comprehensive picture [10] of the natural world.

The literature on critical phenomena and phase transitions is vast, with seminal work dating back several decades. Important studies by Kenneth Wilson, who developed renormalization group theory, have established the foundation for understanding universality and scaling behavior in physical systems [4]. This theory has been essential in

explaining why different systems can exhibit similar behavior near critical points, despite having different microscopic properties. In the context of ecosystems and social systems, the RPS model has been extensively studied, with research highlighting its ability to mimic cyclic dominance and evolutionary strategies. Notable studies have applied the RPS model to various ecological scenarios, demonstrating its versatility in explaining complex interactions and dynamics [13].

The integration of critical phenomena theory with the RPS model in non-equilibrium systems [14, 15] is a novel and growing area of research that aims to establish a bridge between theoretical physics and ecological modeling. We believe that such an interdisciplinary approach is capable of contributing to the understanding of ecosystems dynamics through the application of universality and scaling laws, particularly in the context of the RPS model. However, there is a notable research gap in fully understanding how critical phenomena apply to ecological and social systems within this framework. Current studies tend to focus on either theoretical aspects of critical phenomena or ecological [16] implications of the RPS model, without fully integrating these concepts. This gap highlights the need for more extensive studies to test and refine the theories developed in this area [14], which could significantly advance our understanding of stochastic systems and contribute to the broader field of complex systems research.

This study is the first step in a larger project aiming to categorize RPS systems into different universality classes, inspired by the theory of critical phenomena. This includes the analysis of critical exponents and scaling functions, which are essential for understanding the diverse critical properties of such systems. Our aim here is to investigate how variations in the RPS model control parameters influence the emergence of critical behavior and phase transitions. This involves examining the scaling behavior of the model under different conditions which may help in identifying potentially emerging universality classes.

In order to study the theoretical model, we performed numerical tests to validate the construction of the code based on previous works [17, 18]. Furthermore, the study considers the broader implications of these results, particularly in terms of biodiversity conservation and ecosystem management. The understanding of critical points and phase transitions of RPS systems can improve our strategies for biodiversity conservation and ecological equilibrium. This research aims to make a significant contribution to the physical and ecological sciences by providing a new perspective on the complex and dynamic nature of RPS systems.

In the realm of modern physics, the study of critical phenomena occupies a central role, particularly in the context of phase transitions. These transitions are pivotal in determining the behavior of a myriad of physical systems as they approach their critical points. A quintessential example of this is observed in the behavior of a ferromagnetic nearing

its critical temperature. Here, the magnetization, which serves as the order parameter, progressively diminishes and ultimately vanishes at the critical point, signifying a marked phase transition. Furthermore, this phenomenon is not isolated to the order parameter alone; other response functions, such as constant-field specific heat and isothermal susceptibility, also demonstrate singular behaviors at critical points [19]. The ubiquity of these phenomena across a diverse range of physical systems not only highlights their fundamental nature but also underscores the imperative for an in-depth understanding.

The concept of scaling is a cornerstone principle in the study of critical phenomena. Scaling laws, characterized by specific exponents, are instrumental in elucidating the behavior of physical quantities in the vicinity of critical points [19]. In this thesis we apply a significant manifestation of this concept known as the phenomenon of data collapse, which has received extensive validation through experimental and theoretical studies. This facet of scaling uncovers an inherent simplicity within the complex dynamics of systems at critical conditions [19].

Equally crucial is the concept of universality, which arises from the empirical observation that disparate systems exhibit analogous behaviors near their critical points. This leads to the classification of these systems into universality classes, each defined by distinct critical-point exponents and scaling functions [19]. This aspect of the discussion brings to light the fascinating observation that various physical systems, despite their differences, can display strikingly similar critical behaviors, suggesting a deep-seated commonality in their underlying physics.

The Renormalization group theory offers a comprehensive theoretical framework for understanding the principles of scaling and universality. It introduces the concepts of upper and lower marginal dimensionality, which are crucial in determining the relevance of classical theories for describing critical phenomena. This approach has not only deepened the understanding of scaling and universality but has also paved the way for new concepts and methodologies in the study of critical phenomena [19]. In summary, the exploration of critical phenomena in modern physics, particularly through the lenses of scaling, universality, and renormalization, provides profound insights into the behavior of physical systems near critical points. This study is not only relevant in advancing the understanding of phase transitions but also plays a role in the broader context of physical and biological sciences.

Furthermore, this research paves the way for future interdisciplinary studies, encouraging collaboration between physicists, ecologists, and social scientists. The methodology and findings of this study can be used as a foundation for further research, exploring other complex systems where critical phenomena and stochastic dynamics play a crucial role. By demonstrating the applicability of critical phenomena theory in the RPS model, this study opens new avenues for research, thus broadening our understanding of complex systems.

1.2 Overview

To provide a seamless and guided reading experience, we have implemented a structured framework for this work. Our intention is to ensure clarity and coherence throughout the document. The following ideas have been carefully organized to facilitate a fluid comprehension of the research.

In chapter 1, the **Introduction**: The text begins with an initial discussion on critical phenomena and the RPS model and its significance in understanding complex adaptive systems. It highlights the importance of scaling and universality in RPS dynamics, phase transitions in ecological and social systems, and the relevance of empirical observations and theoretical models. The introduction also touches on stochastic dynamics, fluctuations, applications in biodiversity and conservation, challenges in integrating critical phenomena with RPS, future research directions, and the value of interdisciplinary collaboration.

In chapter 2, the **RPS Model Overview**: This section provides an in-depth look at the RPS model, focusing on population dynamics, biodiversity, and the coevolution of species. It discusses the limitations of deterministic models and the need for a more realistic approach that incorporates stochastic effects. The text uses the example of the side-blotched lizard to illustrate the application of the RPS model in understanding reproductive strategies and their implications for population dynamics.

In chapter 3, the **Critical Phenomena Theory**: This chapter delves into the definition of the critical point, introduction to critical exponents, the scaling hypothesis, analytical framework of the correlation function, and continuous phase transition.

In chapter 4, the **RPS Model Critical Phenomena Analysis**: This part of the text includes a simulation of the RPS model, analysis of the order parameter, evaluation of the correlation function, and a study of self-similarity and critical exponents.

In chapter 5, **Critical Analysis**: We actually apply the theory of critical phenomena within the RPS model. We show in detail how the critical point as well as the critical exponents can be obtained by applying scale transformations to the two-point correlation functions in Fourier space. There we also discuss the relevance of critical phenomena theory in understanding the complex dynamics of ecological interactions and validates the theoretical models used.

In chapter 6, **Summary and Conclusion**: The final chapter summarizes the research findings, emphasizing the application of critical phenomena theory to the RPS model and its implications for theoretical ecology and practical applications like biodiversity conservation. It outlines future research directions, suggesting the use of renormalization group theory to further explore the universality classes of RPS models.

2 RPS Model Overview

2.1 Introduction to the RPS Model

The analysis of population dynamics, with a focus on the comprehension of biodiversity and the coevolution of species, is a significant challenge. In the course of time, several mathematical models have been developed to explain the process of competition between species. Initially, deterministic, even nonlinear, models such as those proposed by Lotka and Volterra [20, 21, 22, 23, 24] and their variants, played a prominent role in this field. These models were limited in their predictions due to the absence of stochastic effects [20]. In view of these limitations, the motivation arises to explore a model that approximates a more realistic condition, where stochastic effects play a predominant role and generic properties can be obtained more precisely [20].

An illustration of this type of interaction can be found in the observation of the side-blotched lizard of the species *Uta stansburiana* [25], a species native to the arid region of the west coast of the United States and northern Mexico. These lizards are characterized by the phenomenon of polymorphism, which is manifested by lateral marks in orange, blue and yellow. These different coloration are directly related to different copulation strategies with females. This observation in nature provides an interesting context to study the RPS model, offering the opportunity to clarify the mechanisms underlying these reproductive strategies and their implications for population dynamics. It is important to emphasize that the complexity of these observations in nature transcends simple prey-predator dynamics.

The males of the species *Uta stansburiana* have three different mark morphologies: orange, blue and yellow, each one with unique copulation strategies [26]. The orange-spotted males, the larger and more aggressive of the three, are ultra-dominant, cover large areas and hold multiple mates, although they often lose their females to the yellow-spotted males. On the other hand, the blue-spotted males, which are intermediate in size, are dominant, occupy smaller territories, and generally have fewer or only one mate, are more effective at protecting their females from the yellow-spotted males. The yellow-spotted males, on the other hand, are similar in coloration to the females and use a strategy of simulated rejection when they invade other territories. They have no territory of their own and occupy large areas that may overlap with those of other lizards. The yellow-spotted males are more successful in copulating with females in the territory of the orange-spotted males. Under certain circumstances, they may adopt the behavior of blue-spotted males. In summary, this population dynamics creates a cycle in which the strategy of yellow-spotted males is superior to the ultra-dominant strategy of orange-spotted males, but inferior to the territorial guarding strategy of blue-spotted males. Conversely, the strategy of the

orange-spotted males is superior to the strategy of the blue-spotted males [25].

The application of deterministic equations to the evaluation of biological systems, such as lizards, presents significant challenges. This is due to the complexity of ecological interactions, which often cannot be adequately described by simple mathematical models. In the case of population dynamics, deterministic equations tend to ignore the influence of stochastic factors and environmental fluctuations which play a crucial role in reality. This simplicity can lead to imprecise and incomplete predictions for complex biological systems.

Therefore, the use of stochastic simulations, becomes essential to capture the nuances and variability inherent in these systems, allowing for a more realistic and comprehensive understanding of their dynamics. In order to deal with the complexity of this kind of problem, we chose to adopt a cyclical predator-prey model using a stochastic lattice simulation with periodic boundary conditions. This model is known in the literature as the RPS model. The RPS describes, in a non-hierarchical way, the interaction between three different species in a generic population, allowing us to explore under what conditions these species can coexist harmoniously within the same ecosystem. The essential interactions within this lattice include movement, reproduction, and predation, where a chosen species can interact with one of its four close neighbors [17, 18, 27]. It is important to note that lizards are only one of the examples found in nature where the RPS model proves applicable, and its usefulness extends to a variety of complex ecological systems and other physical problems in the literature.

If we approach the analysis of such problems from the perspective of the theory of critical phenomena, we can find a wealth of details that allow us to understand the nuances of population dynamics. This approach takes into account the phase transition, a crucial concept in statistical physics that describes the change in the behavior of the system when critical values for some parameters are approached. In the context of the RPS model, this phase transition can be interpreted as a critical point at which populations experience drastic changes in their dynamics. For example, this critical point may lead to the extinction of a species or, alternatively, to the exclusive dominance of a single species, compromising the biodiversity of the ecosystem.

Biodiversity represents the diversity of life in an ecosystem and plays a fundamental role in its stability and resilience. The greater the diversity of species in an ecosystem, the more probable it is that some of them may play a critical role in maintaining ecological balance. In scenarios where biodiversity is compromised, the system may become more vulnerable to ecological perturbations and less able to recover from adverse events [28, 29]. Therefore, understanding how changes in population dynamics affect biodiversity is fundamental for the conservation and appropriate management of ecosystems, as well as for assessing their resilience in the face of environmental and climatic challenges. This multidisciplinary approach, combining critical phenomena theory with stochastic

simulation, represents a valuable advance in the study of complex biological systems.

Over the last few decades, many efforts have been made to develop and improve stochastic models to understand complex biological systems. One of the pioneers using the RPS model in this area was Reichenbach, whose groundbreaking work provided the basis for a more detailed understanding of the dynamics of these systems [27].

2.1.1 Mobility impacts biodiversity in RPS games

In the study by Reichenbach [27], one of the main focuses was the influence of mobility in the lattice on the biodiversity of a system. He defined mobility as being directly proportional to the probability of position exchange between close neighbors, represented by ε, and inversely proportional to the total number of sites of the lattice, represented by N_s. This characterization resulted in the formula $M = 2\varepsilon N_s^{-1}$, which quantifies the mobility of the system. One of the main results of this study was the determination of the critical mobility value, M_c, which was calculated to be approximately equal to $(4.5 \pm 0.5) \times 10^{-4}$. When the mobility of the system exceeds this critical limit, biodiversity is compromised and the system tends to evolve towards a state of uniformity in which only one species survives.

On the other hand, when mobility is maintained under this critical threshold, a completely different scenario is observed. In this case, the species coexist in a stable state, and this equilibrium is accompanied by the formation of spiral waves that evolve over time. These spirals represent the cyclical interactions between the species [27], as described by the RPS model.

Reichenbach's pioneering work not only highlighted the importance of lattice mobility as a determinant of population dynamics, but also demonstrated how the RPS model can be a powerful tool for investigating the complex relationship between biodiversity and species interactions in ecological systems. This approach has provided valuable insights into how mobility can influence the stability and diversity of biological communities, with important implications for understanding and maintaining natural ecosystems. The research of Reichenbach *et al.* [20] also explored the critical limits of mobility, examining the transition between states of diversity and uniformity.

2.1.2 Junctions and Patterns in RPS Models

Later, studies explored these spirals and extended the original model. For example, in [17], researchers investigated population dynamics in a context where the number of species was arbitrary. The aim was to observe how the system behaved in scenarios with even and odd numbers of species. Another relevant study, conducted in [18], used stochastic simulations in a two-dimensional lattice to study the behavior of interfaces

separating different species, with a cyclic predation rule. In these simulations, the presence of partnerships between species was observed. For example, when the number of species was $N = 6$, two partnerships were formed, $\{1, 3, 5\}$ and $\{2, 4, 6\}$, each occupying different regions in the lattice.

In addition, the researchers performed simulations based on a mean-field theory and achieved similar results. These simulations reinforced the conclusion that as the number of species N increases, so does the number of peaceful partnerships. This, in turn, induces the generation of stable dynamical structures at the interfaces, whose complexity increases with N. These observations are consistent in both stochastic lattice simulations and mean-field simulations, in one and two dimensions. The formation of patterns is extremely important for the conservation of biodiversity [30]. The formation of cooperative groups is essential for territorial defense, resulting in the "defeat" and "expulsion" of invaders.

2.1.3 Mobility-Driven Coexistence

The study by De Oliveira and De Moura [31] introduces a groundbreaking continuous model to investigate the dynamics of living organisms, with a particular focus on the role of mobility in the coexistence and spatial distribution of organism clusters. This model marks a significant evolution from previous models by integrating individual and collective mobility parameters and substituting global restrictions with local constraints on population density. The authors uncover a dual role of individual mobility: moderate mobility disrupts cluster formation and endangers population survival, while higher mobility levels aid in population recovery and sustainability. This paradoxical discovery highlights the intricate relationship between movement patterns and population dynamics. The model further reveals that collective, biased movement results in distinct spatial patterns, such as stripe-like states, diverging from the hexagonal symmetry typical in randomly moving populations.

In their analysis, De Oliveira and De Moura [31] provide a nuanced understanding of how mobility influences pattern formation and survival in living systems. The study underscores the delicate equilibrium between reproduction and mortality rates and how these are impacted by the mobility of individuals within a population. The findings have broader implications for comprehending the dynamics of ecological systems, suggesting that mobility is a pivotal factor in the resilience and adaptation of populations. This research enriches the field of ecological modeling by offering insights into the mechanisms driving pattern formation and stability in biological populations, with potential applications in various ecological and biological systems.

2.1.4 Pestilent Species and Stability

Bazeia *et al.* [28] explore the impact of a fourth, pestilent species on a system of three cyclically dominant species, grounded in the framework of evolutionary game theory and using the RPS game-like cyclic dominance as a model. The study investigates the effects of this pestilent species, which exclusively preys on one member of the cyclic trio, on the overall biodiversity and stability of the system. The research employs numerical simulations on a spatial model with four species distributed on a square lattice, following the standard rules of the May-Leonard model for the first three species and a Lotka-Volterra type predation rule for the fourth, pestilent species.

The study described in ref. [28] describes a significant shift in ecological dynamics in its third phase, triggered by an increase in the invasion strength of a newly introduced plague species. This phase is characterized by the disappearance of one of the species, a critical component in the predator-prey relationships of the system, which disrupts the existing balance of cyclic dominance. As a result, one species becomes dominant and dominates the ecosystem in the absence of its predator. The loss of one species not only changes the dynamics of species interactions, but also leads to the disappearance of typical spiral patterns formed by the cyclic trio of red, blue, and yellow species. These patterns, indicative of a balanced ecosystem where no single species is overwhelmingly dominant, are lost, signaling a major change in the biodiversity and ecological stability of the system.

The application of Hamming distance density profiles in this phase of the study is critical to a better understanding of these ecological changes. Hamming distance measures the difference between two system states and provides insight into how changes in one part of the ecosystem can lead to significant overall changes over time. This analytical approach sheds light on the cascading effects following the introduction of the plague species and the subsequent extinction of one species. The result is a new ecological equilibrium characterized by the dominance of one species and the loss of the spiral patterns that previously symbolized a diverse and balanced ecosystem. This phase of the research highlights the complex and often unpredictable consequences of external disturbances, such as the introduction of a new predatory species, on ecological systems, underscoring the delicate nature of biodiversity and the balance within these systems [28].

The research concludes that the presence of a pestilent species can significantly alter the dynamics of cyclically dominant systems. The introduction of a species that preys on only one member of the cyclic trio can lead to unexpected outcomes, such as the survival of the pestilent species resulting in its own extinction. This study enriches the understanding of cyclically dominant systems, highlighting the complex and sometimes counterintuitive nature of these interactions. The findings have implications for understanding biodiversity and the stability of ecosystems where such cyclic dominance is present [28].

2.1.5 Environment-Driven Oscillations in the May-Leonard Model

Bazeia *et al.* [32] delve into the impact of environmental conditions on the dynamics of species competition and coexistence. Based on the May–Leonard model, a mathematical framework for describing non-transitive interactions among competing species, particularly in spatial systems, the study extends the rock-scissors-paper game, where each species is both a predator and prey.

The research focuses on how varying environmental conditions, represented by a local carrying capacity parameter, affect the patterns and dynamics of species interactions. Employing an off-lattice version of the May-Leonard model allows for a more detailed manipulation of environmental conditions. The results indicate that in a benign environment with high population density, rotating spirals composed of competing species become more evident. These spirals and their accompanying time-dependent oscillations of competing species display a scaling law relative to the environmental parameter [32].

The study [32] also examines the role of individual movement and how it influences the spatial distribution and evolutionary outcomes of the species. The model reveals that in harsh environments with limited resources, the local carrying capacity is low, supporting fewer individuals, while in more favorable environments, this capacity is higher. The research highlights the importance of environmental conditions in maintaining biodiversity and the dynamics of cyclic dominance in populations. This work contributes to the understanding of how environmental factors, alongside non-transitive interactions, play a crucial role in the evolution and coexistence of species.

2.1.6 Neighborhood Influence on Cyclic Biodiversity Models

In [33], the authors explore the impact of neighborhood interactions in RPS models of biodiversity. The study focuses on three species evolving under standard rules of mobility, reproduction, and competition, with competition following the RPS game dynamics. The authors utilize the von Neumann neighborhood concept but extend it to include interactions with the nearest, next nearest, and next to next nearest neighbors in three different environments. These environments vary in terms of probability distribution, either equal probability or following power law and exponential profiles. The study reveals that increasing the neighborhood size significantly affects the system's characteristic length. The research also examines scenarios where the cyclic evolution is broken by altering how a specific species competes, leading to the counterintuitive result where the strongest individuals may become the least abundant population.

The methodology [33] involves simulating the time evolution of the system in a square lattice with periodic boundary conditions, where each site is surrounded by a neighborhood of four nearest sites. The simulations consider five distinct scenarios for

mobility rules, including the standard model and models with extended neighborhoods. The study quantifies the spatial behavior using a scalar field representing species in the lattice and the spatial auto-correlation function. The results from the simulations show that the characteristic length of the model is modified by including other neighbors and altering the probability associated with their presence. The study also investigates the abundance or density of species over time, using the discrete Fourier transform to quantify oscillations in species density.

The findings indicate that the characteristic length increases non-linearly with increased mobility and neighborhood size [33]. The characteristic frequency, indicating the number of oscillations in species abundance over time, also depends on the neighborhood size and increases with it. The study also examines the extinction probability, showing that a larger neighborhood lowers the mobility value required to break biodiversity. This research contributes to understanding biodiversity maintenance and offers insights into more realistic models by considering extended neighborhood interactions. The study's implications extend to various ecological and biological systems, providing a deeper understanding of the dynamics governing species interactions and biodiversity.

2.1.7 Cyclic Interactions and Pattern Formations

In [13], the authors delve into the intricate world of pattern formations driven by cyclic interactions, a field that has garnered significant interest due to its implications in understanding biodiversity and ecosystem stability. The review commences by acknowledging the centenary of Lotka's seminal work, underscoring the enduring relevance of non-transitive interactions in ecological and biological systems. The authors provide a comprehensive overview of various systems exhibiting cyclic dominance, ranging from spiral waves in cell colonies to oscillations in salmon populations, thereby illustrating the widespread occurrence of these interactions in nature. The review not only summarizes recent developments in this field but also connects these ecological models to evolutionary game theory in social systems, thereby bridging the gap between biological and social sciences.

The core of the review focuses on two fundamental modeling approaches in the study of cyclic interactions: the Lotka-Volterra (LV) and May-Leonard (ML) models. These models, while conceptually similar, differ in their treatment of species competition and population dynamics. Ref. [13] discusses the nuances of these models, particularly how they handle species coexistence and the conditions under which biodiversity is maintained or jeopardized. The review highlights the critical role of interaction graphs, mobility, and long-range interactions in these models, and how they influence the stability of species coexistence. Additionally, the authors explore the impact of various factors such as spatial heterogeneity, site-specific invasion rates, and environmental randomness on biodiversity,

providing a nuanced understanding of the complex dynamics governing ecological systems.

In the concluding sections, ref. [13] explore extensions of these basic models, particularly those involving more than three species, and the resultant complex dynamics of cyclic dominance. They discuss the formation of alliances among species and the competition for space, emphasizing the importance of initial conditions in simulations. The review ends with an outline of potential future research directions, suggesting areas that could yield deeper insights into the dynamics of socio-ecological systems. This review not only synthesizes recent advancements in the field but also sets the stage for future explorations, highlighting the multifaceted nature of cyclic interactions and their significance in understanding the complexity of ecological and social systems.

2.1.8 Competition Effects on Pattern Formation in RPS game

In their insightful study, Jiang *et al.* [34] delve into the complex dynamics of pattern formation and biodiversity within the framework of the RPS game model, a cornerstone in understanding ecological and evolutionary dynamics. Their research employs a lattice-based model, where individual nodes represent either one of three competing species or vacant sites, to explore the intricate interplay of competition, reproduction, and mobility. The focus is particularly on the competition rate, a critical factor in the dynamics of the system.

The study uncovers several key findings about the dynamics of biodiversity and pattern formation under varying competition rates. A notable observation is the phase transition from a biodiverse state to an absorbing phase, where two species go extinct, heavily influenced by the competition rate. Higher values of competition rate are found to enhance biodiversity but disrupt spatial pattern formation, leading to the fragmentation of macroscopic spirals and the emergence of disordered spatial structures. This disruption is attributed to the prevention of patterns outgrowing the system size, a novel insight into the balance of ecological systems.

Jiang *et al.* work [34] contributes significantly to our understanding of ecological and evolutionary dynamics in cyclically interacting systems. The study highlights the delicate balance between competition rates and mobility in shaping biodiversity and pattern formation. It also reveals that larger system sizes and higher mobility rates increase the critical competition rate p_c, necessary for the stability of single-armed spirals. These findings underscore the complexity of ecological systems and have broader implications for understanding spatial dynamics in both biological and social systems. The research provides a valuable framework for future studies in the field, emphasizing the crucial role of cyclic competition rates in determining spatial pattern formation and biodiversity maintenance.

2.2 Model Simulation Techniques

In the realm of ecological systems, the application of critical phenomena theory, a cornerstone of statistical physics, presents a fascinating avenue for exploration. This theory, which has profoundly impacted our understanding of phase transitions and scaling behavior in physical systems, offers a unique lens through which we can examine the complex dynamics of ecological interactions. Particularly intriguing is the potential application of this theory to the study of cyclic dominance as exemplified by the RPS model.

This work was based on numerical experiments in which we generated our own data sets for analysis, after carefully reviewing the existing literature that addresses the research topic. Data was collected through computer simulations using codes developed by the author, following the RPS model [17, 18, 27] as a guide. These simulations allowed us to estimate the approximate value of the critical movement μ_c, and to explore the dynamics of the system near the transition region.

Our results indicated that below this critical movement threshold, we observed the formation of complex patterns and the formation of species clusters, indicating the presence of diversity (or biodiversity) in the system, a behavior consistent with that described in the literature [27]. In addition, we noticed that the arms of the spiral patterns tend to increase in size as we approach the critical movement. In other words, the structure of these spirals grows until it reaches a point where it exceeds the dimensions of the lattice. When this occurs, the diversity patterns cease to exist and the system enters a state of uniformity. In this process, only one dominant random species survives, while the other two are eliminated.

The initial conditions of our system are a square matrix of dimensions $N \times N$ with periodic boundary conditions and random initialization. Initially, the lattice is filled with a uniform distribution, assigning an equal weight of $\frac{1}{4}$ to each species as well as to the empty spaces. Each cell in the lattice is represented by an integer, denoting individuals of the species, where 1 corresponds to the blue species, 2 to the red species, 3 to the yellow species, and 0 to empty spaces represented by white color.

At each iteration, one cell is randomly selected as the active cell. This active cell has the ability to interact with one of its four nearest neighbors, labeled the passive cells. The possible interactions between the active cell and its neighbors were classified as movement, reproduction, and predation, with probabilities denoted by μ, λ, and σ, respectively.

These interactions have been defined as follows [17]: *Movement*: The active cell and the passive cell exchange positions, represented as $l \odot \rightarrow \odot l$. *Reproduction*: The active cell is duplicated as long as the passive cell is an empty space, represented as $l\otimes \rightarrow ll$. *Predation*: The active cell eliminates the passive cell leaving an empty space, represented by $l(l+1) \rightarrow l\otimes$. Where $\otimes$ symbolizes an empty space, and $\odot$ can represent any species l

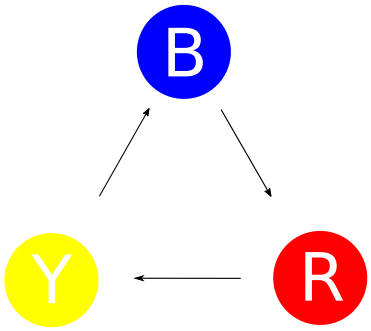

Figure 1 – Scheme of interaction between the three species, with predation to the right.

or an empty space. The RPS model allows the specification of the type of predation, either to the right or to the left. Additionally, it is possible to configure simultaneous predation in both directions. However, for the purposes of this study, we chose to consider only right predation for convenience and simplicity, as illustrated in Figure 1.

A schematic illustration of the interaction rules in the RPS model, shown in Figure 2, provides a clearer understanding of the rules. In Figure 2a shows the initial matrix, which is randomly generated independent of the initial parameters, with equal probabilities assigned to all species and empty spaces. In Figure 2b, the highlighted cells in the rectangle show the active blue cell preying on the passive cell directly above it, leaving an empty space previously occupied by a red species. In Figure 2c shows the selected cells where the active red cell switches positions with the passive cell. And in the Figure 2d shows the marked cells where the active yellow cell reproduces, filling the neighboring empty cell above it.

It is also important to note that we have used tools and techniques from the theory of critical phenomena to analyze the data obtained in the simulations. This integration of tools from the theory of critical phenomena enriched our analysis and contributed significantly to the comprehension of the results obtained.

We developed the code from scratch for data generation and analysis, all implemented in *Python*. Our simulations typically run for 21 days on a computer equipped with two *Intel(R) Xeon(R) CPU E5-2667 v4 @ 3.20GHz* processors, each featuring 8 cores and supporting 2 threads per core. Such a high demand for computer resources is due to the phenomenon known as *critical slowing down* [29], which occurs in the vicinity of the critical point.

In physics, critical slowing down is a phenomenon typically observed near second-order phase transitions, where the relaxation time of a system diverges [29, 35]. This means that the system becomes increasingly slow to respond to external perturbations. Critical slowing down is closely connected to the diverging correlation length near a critical point, which leads to a loss of local equilibrium and an increase in global fluctuations. Consequently, near the phase transition, critical slowing down substantially prolongs the

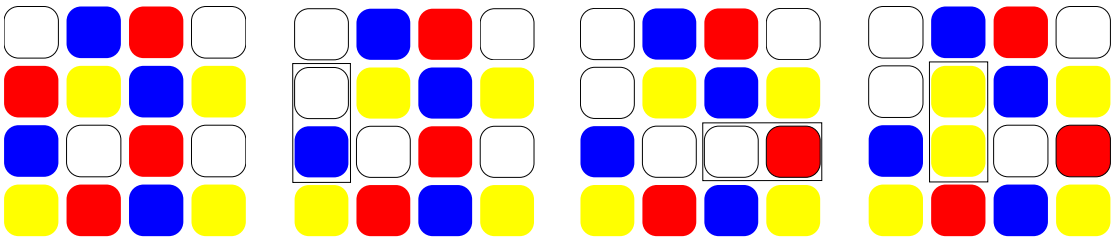

Figure 2 – Illustration of the RPS model interaction rules. **(a)** Randomly generated initial matrix. **(b)** Blue species predate red. **(c)** Red species switch positions with empty space. **(d)** Yellow species occupy an empty site.

relaxation time, thereby decelerating the dynamics of second-order phase transitions [35].

This phenomenon has important implications for the understanding of critical phenomena in various physical systems, such as ferromagnetic, superconductors, and fluids [2]. In particular, critical slowing down can lead to dramatic changes in the dynamics and properties of a system, such as glassy behavior [36, 37] and the formation of self-organized structures. In biological systems it is usually a consequence of the increasing interdependence and connectivity of the system's components as it approaches a critical point [38]. On the other hand, it can also make the system more vulnerable to collapse or catastrophic events [39].

Understanding critical slowing down in biological systems is important for a variety of reasons. It can help us to predict and mitigate the effects of critical transitions, such as ecosystem collapse or disease outbreaks.

Therefore, we believe that the integration of several concepts and approaches makes this work a pioneering effort at the intersection of critical phenomena and complex biological systems. This innovative approach has allowed us to identify critical and universal behaviors in a biological context, providing valuable context for how interactions between species and interspecies can evolve in complex and dynamic environments.

3 Critical Phenomena Theory

3.1 Definition of the Critical Point

Critical phenomena pertain to the characteristic behavior displayed by physical systems in proximity to a critical point, which designates a phase transition point. When a system reaches criticality, it demonstrates universal behavior, wherein distinct properties become decoupled from the specific system particulars and instead rely on a small set of critical exponents. This pursuit is not primarily concerned with identifying a theoretical framework that accurately encompasses experimental data across the entirety of the temperature range, but rather emphasizes the investigation of these critical exponents within a localized region.

One fundamental aspect pertains to the physical phenomena involved, specifically the establishment of significantly extended correlations encompassing an extensive number of constituent particles, which notably emerge and dominate in proximity to the critical point. However, these phenomena are conspicuously absent and diminish in significance as the system diverges considerably from the critical point. Within the current context of investigation, it is imperative to acknowledge the presence of well-defined relationships that exist among the critical exponents. These relationships are derived from fundamental principles inherent in thermodynamics and statistical mechanics, and therefore possess a universal nature that extends beyond the confines of any specific system under consideration.

The critical point is defined by the specific set of conditions at which a phase transition occurs. In the context of critical phenomena, the behavior of a general function, denoted as $f(\varepsilon)$, where,

$$\varepsilon \equiv \frac{x - x_0}{x_0} = \frac{x}{x_0} - 1, \tag{3.1}$$

in the vicinity of the critical point is encapsulated by a set of indices known as critical point exponents. These exponents serve as mathematical descriptors that characterize the scaling properties and critical behavior exhibited by the system. In particular, they provide dimensionless variables that quantify the variations in a relevant physical parameter, *e.g.*, temperature, and elucidate the fundamental nature of the phase transition. As a fundamental assumption, it is presumed that the function $f(\varepsilon)$ maintains positivity and continuity for sufficiently small positive values of ε, and that the limit

$$\lambda \equiv \lim_{\varepsilon \to 0} \frac{\ln f(\varepsilon)}{\ln \varepsilon}, \tag{3.2}$$

exists.

The limit, denoted as λ in equation (3.2), represents the limit behavior associated with the function $f(\varepsilon)$ at its critical point. To express this association concisely, a shorthand notation, namely

$$f(\varepsilon) \sim \varepsilon^{\lambda}, \tag{3.3}$$

is commonly employed, indicating that λ assumes the role of the critical point exponent for the function $f(\varepsilon)$ under consideration. It is crucial to emphasize that the relation $f(\varepsilon) \sim \varepsilon^{\lambda}$ should not be misconceived as implying an equality, *i.e.*,

$$f(\varepsilon) = A\varepsilon^{\lambda}. \tag{3.4}$$

Indeed, the converse is true. In reality, the behavior of a typical thermodynamic function is often more intricate than a simple power-law relationship, *e.g.*, (3.3). Generally, we encounter additional correction terms, leading to functional expressions of the form,

$$f(\varepsilon) = A\varepsilon^{\lambda}(1 + B\varepsilon^{y} + \dots), y > 0. \tag{3.5}$$

The presence of these corrections terms results in a more comprehensive description of the critical behavior exhibited by the system, accounting for the complexities beyond the basic power-law behavior. Such functional expressions allow for a more accurate representation of the behavior of the thermodynamic function near the critical point. Furthermore, it is evident that the definition given in equation (3.2) for a critical point exponent does not discriminate between the functional form presented in equation (3.4) and (3.5).

The relevance of quantifying the critical point exponent, regardless of its inherently reduced information compared to the complete functional form, may rightfully be questioned. Nevertheless, the justification for such focus appears to be grounded in empirical findings, which reveal that in proximity to the critical point, the dominant behavior is governed by the leading terms. This experimental insight provides the basis for employing $log - log$ plots to analyze empirical data, where linear behavior manifests in the vicinity of the critical point. Consequently, the critical point exponent can be ascertained as the slope of this linear region, rendering it a measurable parameter. Therefore, critical point exponents are indeed measurable, unlike the complete function, which may not be directly accessible or measurable due to experimental constraints or inherent complexities.

A second justification for focusing on the critical point is the abundance of interrelations that exist among the critical exponents. These interrelations arise from fundamental principles in thermodynamics and statistical mechanics, transcending the particularities of any individual system. The critical exponents are not isolated quantities but are interconnected through universal scaling relations. These scaling relations reveal deep underlying symmetries and universality classes that govern the critical behavior of diverse physical systems. By studying critical phenomena and the associated critical exponents, we obtain insights into universal properties that are shared by a wide range of systems undergoing

phase transitions. This universality allows us to classify and categorize different systems based on their critical behavior rather than their specific microscopic details. Consequently, critical exponents provide a powerful tool for understanding and characterizing the critical behavior of complex systems. In summary, study the critical point and its associated exponents offers a way to unravel universal principles governing phase transitions, providing a deeper and more general understanding of critical behavior that extends beyond the constraints of individual systems.

3.2 Introduction to Critical Exponents

In the domain of critical phenomena, the PV isotherm, which describes the relationship between pressure and volume in fluids, and the HM isotherm, which characterizes the relationship between magnetic field and magnetization in magnetic systems, are of fundamental importance. These relationships are closely related to the concepts of isothermal compressibility K and isothermal susceptibility χ, respectively. Notably, K and χ are inversely proportional to the slopes of their respective isotherms [2].

A fundamental aspect of these relationships is their behavior as the system approaches the critical temperature T_c. Near T_c, both K and χ tend to diverge, a phenomenon that can be described by the critical exponents. This divergence is expressed mathematically for the fluid case as

$$K \sim |T - T_c|^{-\gamma}, \tag{3.6}$$

and for the magnetic case as

$$\chi \sim |T - T_c|^{-\gamma}, \tag{3.7}$$

where γ is the critical exponent associated with both compressibility in fluids and susceptibility in magnetic systems. This exponent γ characterizes the rate at which K and χ diverge as temperature approaches T_c.

The importance of these equations lies in their ability to capture the sudden changes in physical properties that occur near the critical point. In both fluid and magnetic systems, the divergence of K and χ indicates a state of increased sensitivity to external influences, a characteristic of critical behavior. This divergence is a fundamental feature of phase transitions and provides important information about the nature of critical phenomena [2].

The critical exponent δ is an important parameter in the characterization of the behavior of physical systems at the critical isotherm, in particular at the critical temperature $T = T_c$. This exponent is essential in describing how certain physical quantities, such as pressure and magnetization, deviate from their expected values at the critical point. For a fluid system, the variation of the pressure P relative to the critical pressure P_c is given by

the density ρ and the critical density ρ_c [2],

$$\frac{P - P_c}{P_c^0} \sim \left| \frac{\rho}{\rho_c} - 1 \right|^{\delta}, \tag{3.8}$$

where P_c^0 is the reference pressure, defined as $\frac{kT_c\rho_c}{m}$. This reference pressure is the ideal pressure of the system, where the particles do not interact and both the density ρ and the temperature T are at their critical values, ρ_c and T_c, respectively.

Similarly, in the context of magnetic systems, the relation between the magnetic field H and the magnetization M at the critical temperature is described by the equation

$$\frac{H}{H_c^0} \sim \left| \frac{M_H}{M_c} \right|^{\delta}, \tag{3.9}$$

where H_c^0 is defined as $\frac{kT_c\rho_c}{m_0}$, where m_0 is the magnetic moment per spin, and M_H refers to the magnetization of the system under an applied magnetic field H. This term denotes the critical magnetic field of the system at T_c in an ideal case where there are no inter-particle interactions.

The critical exponent δ thus serves as a fundamental measure for understanding the behavior of systems near the critical point. It describes how the pressure in fluids and the magnetic field in magnetic systems deviate from their non-interacting initial values, P_c^0 and H_c^0, as the system approaches the critical point. The description of δ provides useful information about the response of the system to fluctuations in density and magnetic field near the critical point [2].

The critical exponents ν and η are essential to the study of critical phenomena, in particular to the understanding of the behavior of systems in the vicinity of the critical point. These exponents are closely related to the properties of the pair correlation function $G(r)$ and the correlation length ξ, both of which are important in describing the spatial correlations within a system as it approaches criticality [2].

The correlation length ξ quantifies the strength of the correlation between particles or spins within a system. As the temperature approaches the critical temperature T_c, the correlation length exhibits a divergent behavior, which is expressed by the equation [2],

$$\xi \sim |T - T_c|^{-\nu}, \tag{3.10}$$

where ν is the critical exponent describing the rate at which ξ diverges as T approaches T_c. This divergence indicates the emergence of long-range correlations in the system, a characteristic of critical behavior.

The pair correlation function $G(r)$ is a measure of how the presence of one particle affects another at a distance r. This function is particularly important at the critical temperature $T = T_c$, where it reveals the detailed interaction of particles or spins within

a system undergoing a phase transition. At the critical temperature, $G(r)$ exhibits a power-law decay with distance, which is described by the equation [2],

$$G(r) \sim r^{-(d-2+\eta)}, \tag{3.11}$$

where d is the dimensionality of the system, and η is the critical exponent that characterizes how the influence between particles decays with distance at T_c. The exponent η thus provides important information about the nature and intensity of fluctuations and interactions within the system at the critical point, thereby indicating the emergent collective behavior that is not evident in the individual components of the system.

Thus, in combination with the critical exponent ν, which describes the divergence of the correlation length, η provides a comprehensive approach to the analysis of phase transitions and critical phenomena. These exponents, through their influence on the correlation length or pair correlation function, provide a thorough understanding of the behavior of physical systems near the critical point [2].

So far, our discussion has been based on the static scaling hypothesis, but in order to present the last critical exponent, it is necessary to introduce the dynamic scaling. As a system approaches its critical point, the relaxation times associated with various physical quantities, such as magnetization, specific heat, and susceptibility, diverge. This means that it takes longer for the system to reach equilibrium after a perturbation. In these systems, various physical quantities often exhibit power-law dependencies both on time and length scales. Dynamic scaling theory is used to describe how these scaling properties emerge and how they evolve as a system approaches its critical point. Such a theory is closely related to the more general concept of universality.

When a system is close to a critical point, it displays spatio-temporal self-similarity, which means that its physical properties are invariant under rescaling of both length and time. This self-similarity is described by power-law dependencies, where physical quantities show scaling relations with the correlation length and relaxation time. One of the main features of this subject, which differs from the one discussed up to the present moment, is the timescale, also known as the relaxation time, denoted by τ, which diverges as the system approaches the critical point. The relaxation time characterizes how long it takes for the system to relax to equilibrium after a perturbation. And defined is as [40],

$$\tau \sim |T - T_c|^{-z\nu}. \tag{3.12}$$

As illustrated in Equation (3.12), the dynamic scaling hypothesis postulates that both the correlation length and the relaxation time in a system approaching criticality follow power-law dependencies. Consequently, critical exponents like ν and z become interrelated through scaling relationships, often arising from inherent symmetries and constraints within the system. Therefore, the complete form of equation (3.11) is, in fact [40]

$$G(r) \sim r^{-u}, \tag{3.13}$$

with u related to the critical exponent by $u = d + z - 2 + \eta$.

In classical systems, the dynamic exponent z is often equal to zero, thus emphasizing the static character of such transitions. In contrast, in quantum systems, the value of z can be different from zero, indicating a different scaling behavior of correlations in time as the system approaches a quantum phase transition. So, while the general expression for $G(r)$ is applicable to both classical and quantum systems, the specific value of the dynamic exponent z can vary depending on the type of system and the nature of the phase transition.

In a nutshell, we can summarize the subject addressed in the previous sections through a Table 1.

Table 1 – Summary Critical Exponent.

Critical Exponent	Relationship Among Variables	Brief	Interval
δ	$\frac{P-P_c}{P_c} \sim \psi^{\delta}$	Related to the order parameter ψ	$T = T_c$
η	$G(r) \sim r^{-u}$	Related to correlation function decay	$T = T_c$
γ	$\chi \sim \lvert T - T_c\rvert^{-\gamma}$, $K \sim \lvert T - T_c\rvert^{-\gamma}$	Related to susceptibility (or compressibility)	$T < T_c$
ν	$\xi \sim \lvert T - T_c\rvert^{-\nu}$	Related to correlation length decay	$T < T_c$
z	$\tau \sim \lvert T - T_c\rvert^{-z\nu}$	Related to relaxation time decay	$T < T_c$

Source: Produced by Author.

3.3 The Self-Similarity and Scaling Hypothesis

The main idea behind the scale hypothesis is that physical systems exhibit certain scaling properties near critical points. These scaling properties imply that the behavior of the system remains qualitatively the same when its size is rescaled by a factor. In other words, the properties of the macroscopic system depend only on the ratio of relevant length scales, not on the absolute length scales themselves. The scale hypothesis allows us to describe the critical behavior of a system in terms of critical exponents, which are

characteristic numbers that govern how certain properties diverge or become singular at the critical point.

Furthermore, the scale hypothesis implies that critical exponents can be related to each other through scaling relations, reducing the number of independent exponents needed to characterize a critical system. This relationship between critical exponents is a powerful tool in the study of critical phenomena, because it allows us to make predictions and understand the behavior of physical systems near their critical points without the need for detailed microscopic knowledge [2].

In the context of critical phenomena, the concept of self-similarity emerges as a fundamental concept, expressing the idea that the structure and patterns of a system are invariant over a wide range of scales of observation. Most commonly observed near critical points, self-similarity denotes a state in which traditional metrics of scale and dimensionality become obsolete, giving way to fractal-like properties. This phenomenon is not merely a geometric curiosity, but a profound indication of underlying symmetries and universal behaviors [41]. It plays a crucial role in the theoretical understanding of phase transitions, where the scale-invariant nature of fluctuations critically influences the macroscopic properties of the system. Self-similarity is not only a descriptive property, but a fundamental principle that underlies the scaling laws and universality classes that characterize the behavior of systems at their critical points [41].

One illustrative example of self-similarity occurs with fractals [41, 42, 43, 44, 45, 46], which are patterns that exhibit self-similarity across scales [46, 47, 48, 49, 50], and they are present in various forms around us [46, 51, 52, 53, 54]. Scale invariance means that if a part of the system is scaled up to the size of the whole system, there is no detectable difference between the scaled-up part and the original system. This phenomenon is a classic example of self-similarity, which is illustrated in fractal structures, as shown in the Figure 3. These fractals, where each fragment reflects the whole structure, exemplify the principle of self-similarity inherent in systems at criticality [55].

In the study of critical phenomena, both experimental and theoretical research has confirmed the notion that exponent inequalities often manifest as equalities [2]. This intriguing observation invites a full explanation. While a rigorous proof that transforms these inequalities into equalities remains beyond the reach of this thesis, an alternative method, known as the static scaling law or homogeneous function approach can be applied [2]. This method relies on a fundamental assumption about the form of a correlation function. It introduces functional relationships between the critical exponents, limiting the number of independent critical exponents through exponent equivalence [40]. Despite being outside the scope of this thesis, renormalization group theory can provide an explanation for the scaling hypothesis [1, 4, 6]. In renormalization group theory, the idea is to consider the system at different length scales and observe how its properties change as we zoom in

(a) Canopy Tree (b) Barnsley Fern (c) Sierpiński Triangle

Figure 3 – **(a)** Canopy Tree: A fractal canopy is a type of fractal tree formed by repeatedly splitting line segments into smaller parts at varying angles and lengths, creating an infinitely branching structure. This iteration of the fractal canopy has been modified with specific adjustments to branching angles and segment lengths, fine-tuning its structure to more closely mimic the aesthetics of a real tree. **(b)** Barnsley Fern: The Barnsley Fern is a fractal resembling a natural fern, created through iterative affine transformations, exemplifying how repetitive mathematical processes can produce complex, organic patterns. **(c)** Sierpiński Triangle: The fractal described is a fixed set with an overall equilateral triangle shape, repeatedly divided into smaller equilateral triangles, forming a symmetrical and intricate pattern. Source: Produced by the author.

or out. The key insight is that the behavior of a system at a particular length scale can be described in terms of effective parameters that capture the average behavior of the system at that scale.

Furthermore, the scaling hypothesis extends beyond simply establishing relations between critical exponents to make specific predictions about the form of the equation of state. These predictions, which derive from statistical scaling considerations, have been substantially supported by a range of numerical and experimental studies [2]. This convergence of theoretical predictions with empirical findings not only reinforces the validity of the scaling hypothesis, but also demonstrates its importance in providing a coherent approach to understanding the complex dynamics at work in critical phenomena. The consistency of these theoretical constructs with experimental data is a demonstration of the robustness of the scaling approach in unraveling the intricate nature of critical points.

The assumption of homogeneity of a function imposes significant restrictions on the properties of the function, which shape the mathematical behavior of the function in a specific and predictable form. We shall now examine a particular aspect of homogeneous functions that is essential to our analysis. Consider a homogeneous function f of two variables, defined as follows

$$f(\alpha^a x_1, \alpha^b x_2) = \alpha f(x_1, x_2), \tag{3.14}$$

where α^a and α^b are scaling factors with $\alpha > 0$. This equation encapsulates the essence of homogeneity: the value of the function scales in a well-defined way when each of its arguments is scaled. The exponents a and b are important parameters in this context, determining the rate at which the value of the function increases or decreases under scaling transformations.

As the equation (3.14) is valid for any positive value of the scaling parameter α, it remains valid for a particular choice, such as $\alpha = x_2^{-\frac{1}{b}}$. This substitution leads to the expression,

$$f(\frac{x_1}{x_2^{\frac{a}{b}}}, 1) = x_2^{-\frac{1}{b}} f(x_1, x_2), \tag{3.15}$$

where the left side of the equation (3.15), $f(\frac{x_1}{x_2}, 1)$, is essentially a function of two variables, where the second variable is set to unity. This observation allows us to simplify the expression by introducing a function of a single variable, defined as

$$F(y) \equiv f(y, 1), \tag{3.16}$$

so by combining the equations (3.15) and (3.16), we get the following result

$$f(x_1, x_2) = x_2^{\frac{1}{b}} F(\frac{x_1}{x_2^{\frac{a}{b}}}). \tag{3.17}$$

Therefore, all functions $f(x_1, x_2)$ that satisfy the structure of the equation (3.14) can be rewritten according to the equation (3.17). Similarly, functions that satisfy the form of equation (3.17), where $F(y)$ is an arbitrary function as defined in equation (3.16), also satisfy equation (3.14). In essence, functions that can be represented by either the equation (3.14) or the equation (3.17) are considered as homogeneous functions. In our case, the static homogeneous hypothesis states that the correlation function is a generalized homogeneous function [2].

3.4 Correlation Function

In the context of critical phenomena, the correlation function, often denoted as $G(r)$ or $G(k)$, quantifies the statistical correlations or fluctuations between different points in a system as a function of their spatial separation r. It provides information about how the properties of one point in the system are related to those at other points, especially in the vicinity of a phase transition.

For instance, the correlation length ξ emerges as a fundamental quantity related to the decay of $G(r)$. As the separation r increases, the correlation function $G(r)$ typically decays, indicating that correlations between distant points in the system become weaker. Near the critical point, the rate of this decay is determined by critical exponents associated with the system. Correlation function becomes scale-invariant near the critical point, this

scale invariance implies that the system exhibits similar behavior regardless of the length scale being considered. This property is important in characterizing the universality class of the phase transition, which groups different physical systems based on their common critical behaviors despite variations in microscopic details.

Prior to discussing the properties of the correlation function, the focus of this analysis lies in the examination of the average values of variables of typical physical systems. To do so, let us focus initially on density, defined as [2],

$$n(\mathbf{r}) \equiv \sum_{i=1}^{N} \delta(\mathbf{r} - \mathbf{r}_i), \tag{3.18}$$

at a given point $\mathbf{r}$ in the fluid, $\mathbf{r}_i$ denotes the spatial coordinate of the ith particle, and where N is a total number of system particles. In a uniform system, $\langle n(\mathbf{r})\rangle$ is position-independent, and thus, it can be expressed as the ratio between the total number of particles and the total volume of the system [2],

$$\langle n(\mathbf{r})\rangle = \langle \frac{N}{V} \rangle \equiv n, \tag{3.19}$$

where V is the total volume of the system and $\langle . \rangle$ is the ensemble average.

A quantification that provides a more comprehensive representation of the microscopic properties of the system is denoted as $\langle n(\mathbf{r})n(\mathbf{r}')\rangle$. This quantity is proportional to the probability of observing a particle at the position $\mathbf{r}$ given the presence of a particle at the position $\mathbf{r}'$. Accordingly, $\langle n(\mathbf{r})n(\mathbf{r}')\rangle$ serves as a measure of conditional probability, capturing the statistical correlation between particle occurrences at distinct positions within the system.

Thus, in order to measure the fluctuations in density from their average value, we can define the density-density correlation function, also known as the correlation function. This function serves as a tool to characterize the statistical correlations between density fluctuations at different positions within the system,

$$G(\mathbf{r}, \mathbf{r}') \equiv \langle [n(\mathbf{r}) - \langle n(\mathbf{r})\rangle][n(\mathbf{r}') - \langle n(\mathbf{r}')\rangle]\rangle \tag{3.20}$$

Spatial uniformity, also known as spatial homogeneity [2], denotes a characteristic of a system where its macroscopic properties or physical attributes remain invariant at every point in space. In other words, the system exhibits a uniform distribution of its properties across its entire spatial domain, devoid of any variations or spatial gradients. In a spatially uniform system the macroscopic variables, *e.g.*, density and temperature, remain constant across positions. This assumption is frequently behind investigations of phase transitions, critical phenomena, and statistical mechanics in extensive systems where the range of spatial fluctuations are considered insignificant relative to the overall size of the system. Given the assumption of spatial uniformity in our system, indicating

translational invariance, we shall express $G(\mathbf{r}, \mathbf{r}') \to G(\mathbf{r} - \mathbf{r}')$. Moreover, it follows that $n(\mathbf{r}) = n(\mathbf{r}')$, enabling us to rewrite the equation (3.20) in an equivalent form,

$$G(\mathbf{r} - \mathbf{r}') = \langle n(\mathbf{r}) n(\mathbf{r}') \rangle - n^2. \tag{3.21}$$

As the distance $|\mathbf{r} - \mathbf{r}'|$ tends to infinity, the probability of finding a particle at $\mathbf{r}'$ becomes independent of the events occurring at $\mathbf{r}$, implying that the densities become uncorrelated. Hence, as the spatial separation between points $\mathbf{r}$ and $\mathbf{r}'$ becomes increasingly large, the statistical correlation between particle occurrences at these positions decreases, resulting in the loss of correlation between densities. As a result,

$$\langle n(\mathbf{r}) n(\mathbf{r}') \rangle \to n^2. \tag{3.22}$$

Finally, it is important to remark that limit $q \to q_c$, with q denoting a general control parameter and q_c representing the value at its transition can be considered. In a similar way to the limit $T \to T_c$, *i.e.*, the analysis is not necessarily restricted to the temperature. Any thermodynamic quantity can be decomposed into a regular part, which remains finite, along with a singular part that encapsulates all of its singularities [56]. Hence, for values of q close to q_c, such a singular part dominates the properties of the correlation function [57]. More specifically, for $q \to q_c$, the correlation function can be expressed [58] as equation (3.11).

3.5 Continuous Phase Transition

The description of second-order phase transitions is often elucidated in terms of symmetry breaking at the transition point. In order to quantitatively characterize the alterations in these thermodynamic conditions, we can introduce the concept of order parameter. This physical quantity undergoes remarkable modifications as the transition occurs. Second-order phase transitions are also referred to as continuous phase transitions. In this classification, continuous phase transitions are further divided into different universality classes based on the underlying symmetry of the order parameter and the critical behavior near the transition point. The concept of universality and critical exponents plays a central role in this classification. It is characterized by a gradual change in the characteristics of a system as it passes between different phases. The order parameter of the system or its derivatives do not change abruptly or discontinue during a continuous phase transition. Instead, the transition occurs smoothly and the characteristics of the system change depending on external factors such as pressure or temperature change.

A continuous phase transition is formally described by the non-analytic behavior of a thermodynamic potential, such as the free energy or internal energy, as a function of the control parameters, *e.g.*, temperature, pressure. One or more thermodynamic potential

derivatives with respect to the control parameters become singular at the transition point, signaling the start of different phase. These singularities exhibit power-law behavior, and the corresponding critical exponents control the divergence of various thermodynamic parameters as the transition point is approached. Therefore, a continuous phase transition occurs when a system change smoothly from one phase to another as external factors change, without an abrupt change in its order parameter or its derivatives. The thermodynamic potential of this behavior is therefore non-analytical.

The critical values of the system parameters, in which the phase transition occurs, delineate the limits that demarcate the distinct phases within the space of the control parameters. Phase transitions are precisely characterized as region in the control parameter space where the thermodynamic potential exhibits non-analytical behavior [40]. The important behavior near the transition point is encompassed by a restricted set of universal exponents and functions, which is a universal property of continuous phase transitions. These universal characteristics transcend the details of the system under investigation, embracing a wide range of phenomena from fluid dynamics to magnetism.

Changes in the symmetry of the system are often involved in continuous phase transitions. A typical example is the continuous phase change that occurs in ferromagnetic materials from a magnetized phase with a preferred direction to a non-magnetized phase with no preferred direction. This change in symmetry is associated with the appearance of new collective behaviors near the critical point [40]. The ferromagnetic-paramagnetic transition in materials, and the super fluid transition in liquid helium [2, 59] are examples of continuous phase transitions. Continuous phase transitions can be observed experimentally using a number of methods [2, 37, 60, 61] among them measuring the heat specificity, susceptibility, and correlation lengths. Additionally, modern techniques such critical opalescence [2] and neutron scattering [62, 63] offer insight into the behavior of systems close to critical points.

The selection of an appropriate order parameter is commonly determined by its usefulness and is normally set to disappear in the symmetric phase, while manifesting a non-zero value in the non-symmetric phase [40]. Some examples of order parameter could be the density in solid-liquid or liquid-gas transitions, liquid magnetization which is important in the field of ferromagnetic systems. It is noteworthy that depending on the specific system under investigation, the order parameter can be a complex number, a vector or even a tensor. This inherent adaptability underscores the variety of characteristic ways in which the order parameter can encapsulate the inherent aspects of the studied system.

Considering the scaling hypothesis, the interdependence between the exponents can be simplified, leading to a concise formulation of the scaling law [40, 64], as shown

below:

$$2 - \alpha = \nu(d + z), \tag{3.23}$$

$$\alpha + 2\beta + \gamma = 2, \tag{3.24}$$

$$\beta + \gamma = \beta\delta, \tag{3.25}$$

$$\nu(2 - \eta) = \gamma. \tag{3.26}$$

The concept of symmetry breaking is introduced to explain the transition from disordered to ordered phase. For systems with phase symmetry, it is possible to introduce a complex scalar field,

$$\psi = Ae^{i\theta}, \tag{3.27}$$

where A represents an amplitude and θ denotes a phase. Symmetry breaking refers to a fundamental change that occurs without any external influence. In our case, it is the process by which the initially indeterminate phase θ of the complex wave function ψ becomes well-defined in the ordered phase. The disordered phase manifests itself as the average of ψ assumes the value of zero, due the indetermination of the phase θ. The ordered phase establishes a well-defined phase value θ, thus generating a remarkable change in the behavior and macroscopic properties of the system.

The manifestation of spontaneous symmetry breaking gives rise to the selection of a particular non-vanishing value by the phase parameter. This preference emerges as a consequence of infinitesimal external perturbations acting on the system. Within symmetric phase, each discrete microscopic configuration is intrinsically associated with a comprehensive set of configurations, collectively sharing an identical energy value while differing only in the phase factor. According to the Boltzmann ergodic hypothesis, which postulates the equivalence of the time average and the ensemble average, it becomes evident that, in a steady state, system configurations exhibiting equivalent energy levels maintain a distribution of equivalent probability and therefore an equitable population. As a result, this leads to the predominant result of $\langle\psi\rangle = 0$, denoting the absence of an order parameter. Thus, the occurrence of an ordered phase would be theoretically impossible due to this convergence of principles. The resolution of this apparent paradox is due to the peculiarities of infinite systems, in the thermodynamic limit.

Boltzmann ergodicity is the idea that a system in equilibrium will explore all of its accessible microstates over time. In other words, it suggests that if you wait long enough, a system will visit all its possible settings. However, ergodicity breakdown refers to situations where this assumption is not valid and the system gets stuck in specific regions of phase space, delimited by the expression (3.27), preventing it from exploring all possible states [40].

The breakdown of ergodicity can have important implications, especially in complex systems and systems with long-range interactions. This can lead to imbalance behavior,

e.g., consider a system that exhibits hysteresis. As the system goes through cycles of changing inputs, it may not return to the same states it previously occupied. This output of revisiting the same states indicates an ergodicity violation, where the system fails to explore its entire configuration space. The occurrence of hysteresis can be a manifestation of ergodicity breakdown, as the behavior of the system is influenced by its history and the path it has taken in its state space [2]. In the field of neuroscience, neural lattices can exhibit ergodicity breakdown [65], with certain neural firing configurations being more likely than others due to complex connectivity patterns. Additionally, financial markets may exhibit a breakdown in ergodicity in the context of the economy. Due to information asymmetry, market prices may not fully explore all possible price paths, which could result in volatility clustering or persistent patterns [66]. Therefore, this concept is relevant in the study of critical phenomena because phase transitions usually involve the emergence of new macroscopic behaviors as a system moves through different phases.

4 RPS Model Critical Phenomena Analysis

4.1 RPS Model Simulation

In our implementation of the RPS model, the system is initialized on a two-dimensional square lattice with dimensions $N \times N$, where $N = 256$, with periodic boundary conditions. For the purpose of optimizing computational resources, the chosen lattice size has proven to be adequate for the analysis of the phenomena of interest. Given that the study involves phase transitions, it is expected that larger lattices will require more extensive computational times in order to describe the system in the vicinity of a critical point, since correlation times diverge in such regions. This lattice is randomly populated by three distinct species and empty sites. Each site in this lattice is constrained to be either unoccupied or singly occupied by one of the aforementioned species. As the system undergoes its temporal evolution, an active cell, a site occupied by one of the three species, may engage in interactions with one of its four nearest neighbors, here referred to as passive cells.

The scope of possible interactions for each active cell is confined to movement, reproduction, or predation. The total generation is given by $t_N = 2N^2$, which means that each site with an active cell was visited at least $2N^2$ times. In the context of our computational simulations, during each generation step, denoted by t_i, the lattice is scanned to identify positions occupied by active cells, while empty spaces are disregarded. This process ensures that all active cells have the opportunity to interact with their nearest neighbors. An example of the initial configuration is shown in Figure 4.

In the simulations, the control parameter is represented as movement, denoted by μ, and ranges from approximately 0 to 1. When μ is close to zero, the system exhibits extremely slow dynamics, resulting in the formation of species clusters. Conversely, as μ approaches one, the dynamics becomes much faster, and it is in this region that we observe signs of symmetry breaking in the population ratios, which means that we are close to the critical point. Although we were not able to obtain the exact value of the critical point, since such a task could only be exactly performed for an infinite lattice running for an infinitely long time, we estimate it to be at $\mu_c \sim 1$. As we approach $\mu \sim 1$, long-range fluctuations become increasingly pronounced, amplifying errors due to numerical instabilities. It is important to emphasize that our inability to obtain the exact value of μ_c does not affect the validity of our analysis. Our study focuses primarily on the region in the vicinity of the critical point, rather than strictly on the critical point itself. In the intermediate range between these extremes, complex spiral patterns emerge.

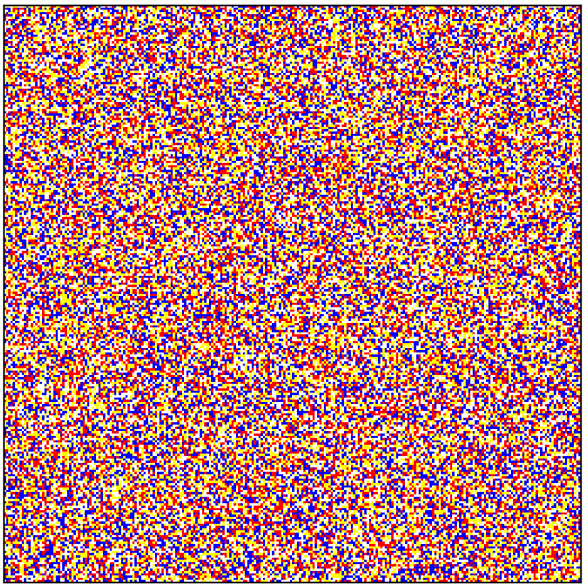

Figure 4 – In the initial configuration of the system, a uniform distribution is maintained for all species (1, 2, and 3) and empty spaces, each occupying a quarter of the total space, $\frac{1}{4}N^2$. This distribution remains constant regardless of the control parameters. In this illustration, blue corresponds to species 1, red to species 2, yellow to species 3, and white to empty space. Source: Produced by the author.

To investigate the universality of critical behavior of the system, we performed two sets of simulations with different parametric settings. This approach is intended to confirm that the behavior of the system exhibits the same critical exponents as it approaches the critical point, regardless of the specific trajectory in parameter space. In the first set of simulations, we used a simultaneous variation of both the predation σ and reproduction λ parameters governed by the relation

$$\sigma = \lambda = \frac{\mu}{2}. \tag{4.1}$$

In the second one, we keep the ratio so that the predation parameter is twice as high as the reproduction value

$$\lambda = \frac{\mu}{3}, \tag{4.2}$$

$$\sigma = 2\lambda, \tag{4.3}$$

for all simulations, such that the relationship

$$\mu + \sigma + \lambda = 1, \tag{4.4}$$

is consistently true.

As the system evolves temporally for $\mu < \mu_c$, distinct spatial patterns begin to emerge. This system configuration is categorized as the diversity regime or, the symmetric phase. In this regime, species coexist and exhibit periodic oscillations in their respective population abundances.

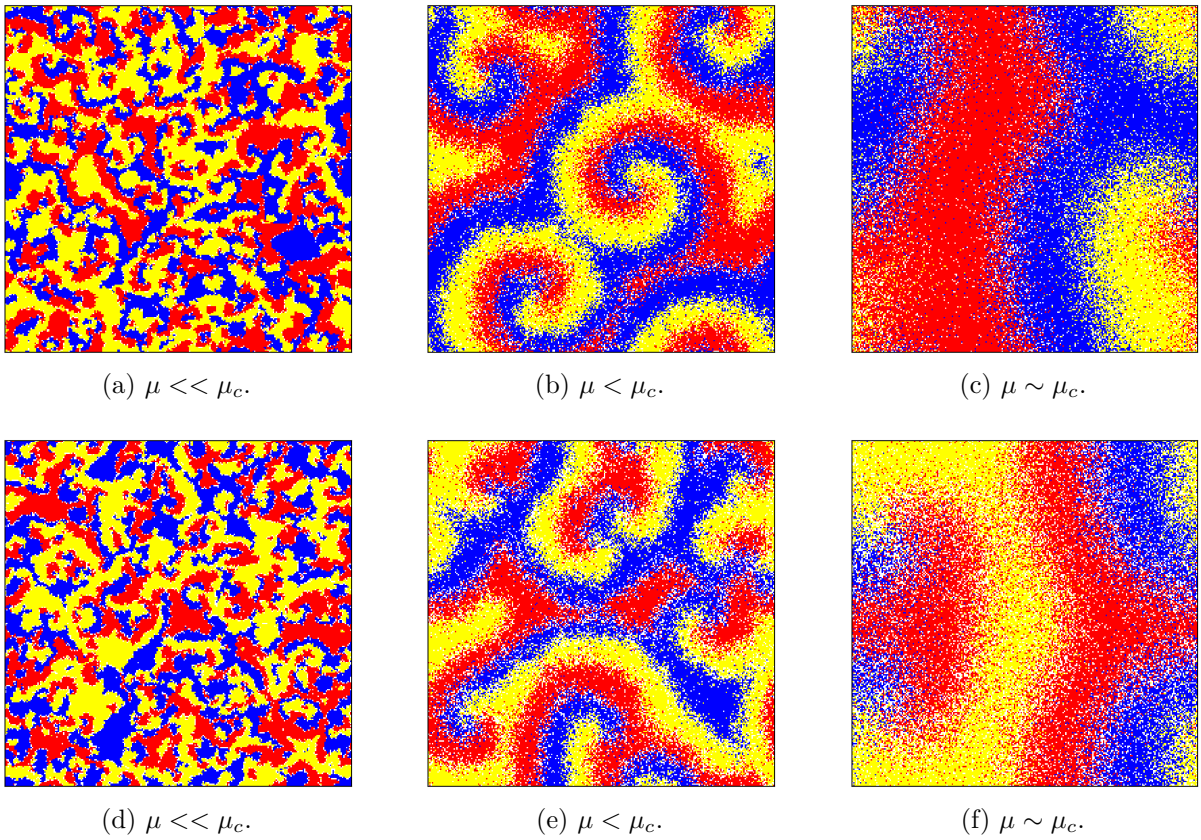

(a) $\mu << \mu_c$. (b) $\mu < \mu_c$. (c) $\mu \sim \mu_c$.

(d) $\mu << \mu_c$. (e) $\mu < \mu_c$. (f) $\mu \sim \mu_c$.

Figure 5 – Spatial distribution patterns of competing species under varying control parameters μ in the diversity regime. In these visualizations, red, blue and yellow color markers indicate the three different species, while unoccupied regions are indicated by white spaces. **(a)** and **(d)** Cluster formation pattern. **(b)** and **(e)** Complex spiral formation pattern **(c)** and **(f)** Flat wavefront-like spatial patterning. The simulation parameters for each scenario are $\mu = 0.0100, \sigma = \lambda = 0.4950$ corresponding to panels (a); $\mu = 0.7347, \sigma = \lambda = 0.1326$ for (b); $\mu = 0.9617, \sigma = \lambda = 0.0192$ for (c); $\mu = 0.0100, \sigma = 0.6600, \lambda = 0.3300$ for (d); $\mu = 0.7347, \sigma = 0.1769, \lambda = 0.0884$ for (e), and $\mu = 0.9673, \sigma = 0.0218, \lambda = 0.0109$ for (f). Source: Produced by the author.

In Figures 5a and 5d it is observed that when the parameter μ is significantly distant from the critical point, the species within the model are organized into distinct clusters. As μ approaches the critical point, a change in the spatial structure becomes evident with the emergence of complex spiral formations, as shown in Figures 5b and 5e. In particular, as μ approaches the critical point, there is an increase in the length of these spiral arms, eventually taking on dimensions comparable to the lattice size itself. This phenomenon is illustrated in Figures 5c and 5f, where the presence of a flat wavefront is also seen. In the Figure 5, the system exhibits evenly distributed population sizes that persists until it reaches a threshold of instability. This threshold marks a critical point where the system transitions to a state where a single species occupying the entire lattice, *i.e.*, it exhibits a symmetry break from a symmetric phase to a non-symmetric one.

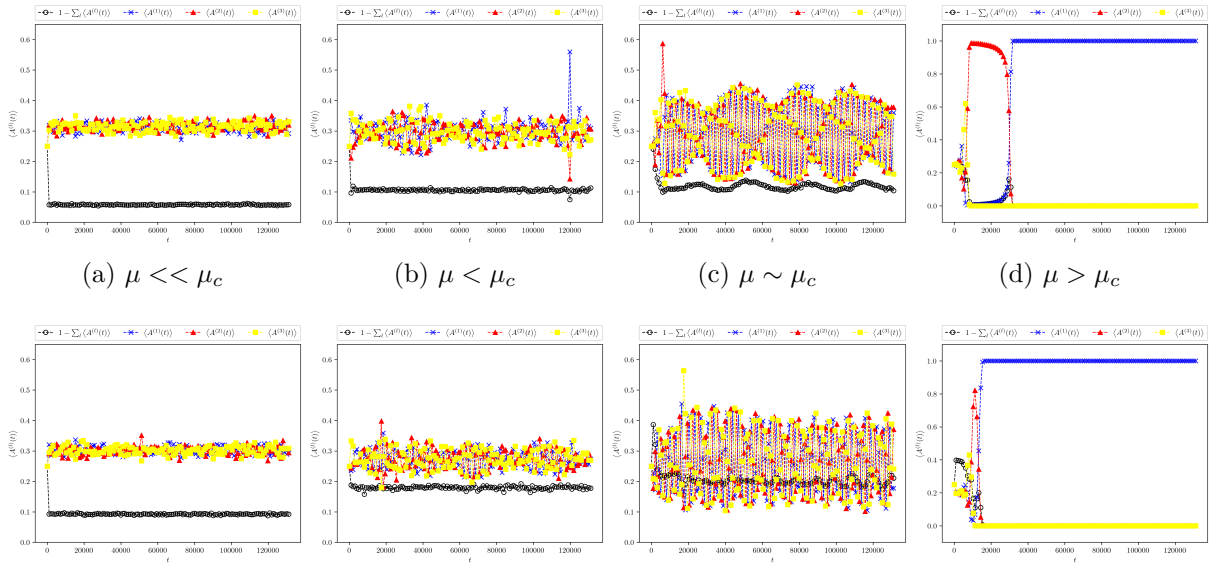

(a) $\mu << \mu_c$ (b) $\mu < \mu_c$ (c) $\mu \sim \mu_c$ (d) $\mu > \mu_c$

(e) $\mu << \mu_c$ (f) $\mu < \mu_c$ (g) $\mu \sim \mu_c$ (h) $\mu > \mu_c$

Figure 6 – Average species abundance for each generation step. Behavior of $\langle A^{(l)}(t)\rangle$ for each species l, and empty space in the diversity and uniformity regimes following a symmetry-breaking phase transition. The simulation parameters for each scenario are $\mu = 0.0100, \sigma = \lambda = 0.4950$ corresponding to panels **(a)**; $\mu = 0.7347, \sigma = \lambda = 0.1326$ for **(b)**; $\mu = 0.9617, \sigma = \lambda = 0.0192$ for **(c)**; $\mu = 0.9872, \sigma = \lambda = 0.0064$ for **(d)**; $\mu = 0.0100, \sigma = 0.6600, \lambda = 0.3300$ for **(e)**; $\mu = 0.7347, \sigma = 0.1769, \lambda = 0.0884$ for **(f)**; and $\mu = 0.9673, \sigma = 0.0218, \lambda = 0.0109$ for **(g)**, and $\mu = 0.9872, \sigma = 0.0085, \lambda = 0.0043$ for **(h)**. Source: Produced by the author.

In order to monitor temporal evolution and quantify the distribution of species and empty spaces within the lattice, we can measure the species abundance. This abundance is defined as the quantity of a species at a specific generation step, relative to the total number of sites. Therefore, for each generation step t_i and for each species, l, where $l = 1, 2, 3$, we associate a real scalar field $A^{(l)}(\mathbf{r}, t)$, where $\mathbf{r}$ denotes the spatial coordinates of sites in the lattice, and the lattice spacing is $\Delta r = 1$. This field takes on the value 1 if species l is present at the site, or 0 otherwise. Therefore, we can express the average species abundance l at time t as follows,

$$\langle A^{(l)}(t)\rangle = \frac{1}{N^2}\sum_{\mathbf{r}} A^{(l)}(\mathbf{r}, t). \tag{4.5}$$

Here, $\langle . \rangle$ denotes the ensemble average.

In the regime characterized by species diversity, we observe that the average abundances of each species tend to oscillate roughly around a value of $\frac{3}{10}N^2$, while the abundance of empty spaces consistently oscillates around $\frac{1}{10}N^2$. This pattern holds regardless of the values of μ, as shown by the data in Figures 6a, 6b, 6e, and 6f. The figures 6c and 6g illustrate the faster dynamics of interactions between species. In addition, the figures 6d and 6h show that as μ approaches the critical point, we observe evidence

of symmetry breaking in the system. In this regime, a single species fills all sites in the lattice, while the others are extinct.

4.2 Order Parameter Analysis

For a comprehensive understanding of a phase transition, it is essential to define the order parameter. In the field of condensed matter physics and the study of phase transitions, the order parameter is instrumental in describing the symmetry-breaking behavior of a physical system as it transitions from one phase to another. The order parameter is a quantifiable measure that reflects the degree of order or organization within the system, providing insight into the degree of symmetry breaking and organization within the system undergoing a phase transition. By exhibiting distinct values or behaviors in each phase, the order parameter serves as a distinguishing feature between different phases.

Essentially, it quantifies the macroscopic properties of the system that change as it transitions between phases. For example, in the context of a ferromagnetic phase transition, the order parameter is often represented by magnetization. This quantity represents the average magnetic moment per unit volume of the material. As the material transitions from the paramagnetic phase (disordered magnetic moments) to the ferromagnetic phase (ordered magnetic moments aligned in the same direction), the magnetization undergoes a significant change, and this change serves as the order parameter. In a liquid-gas critical point scenario, the order parameter can be related to density fluctuations. Near the critical point, the density of the substance fluctuates significantly, and the order parameter reflects the extent of these fluctuations.

Here, the order parameter is defined through a set of fields $\psi^{(n)}(\mathbf{r},t)$, defined by a discrete Fourier transform of $A^{(l)}(\mathbf{r},t)$ with respect to the index $l=1,2,3$, *i.e.*,

$$\psi^{(n)}(\mathbf{r},t)=\sum_{l}A^{(l)}(\mathbf{r},t)e^{i\frac{2\pi}{3}nl}, \tag{4.6}$$

where $n=0,1,2$. The result is the three fields,

$$\psi^{(0)}(\mathbf{r},t)=A^{(1)}(\mathbf{r},t)+A^{(2)}(\mathbf{r},t)+A^{(3)}(\mathbf{r},t), \tag{4.7}$$

and

$$\psi^{(1)}(\mathbf{r},t)=A^{(1)}(\mathbf{r},t)e^{\frac{2\pi}{3}i}+A^{(2)}(\mathbf{r},t)e^{\frac{4\pi}{3}i}+A^{(3)}(\mathbf{r},t)e^{2\pi i}, \tag{4.8}$$

$$\psi^{(2)}(\mathbf{r},t)=\psi^{*(1)}(\mathbf{r},t), \tag{4.9}$$

and for simplicity we will define $\psi(\mathbf{r},t)=\psi^{(1)}(\mathbf{r},t)$. Analyzing the equations (4.7) and (4.8), we observe that

$$\psi(\mathbf{r},t)\psi^{*}(\mathbf{r},t)=\psi^{(0)}(\mathbf{r},t)\psi^{(0)}(\mathbf{r},t), \tag{4.10}$$

due to the definition of $A^{(l)}(\mathbf{r},t)$, where it is equal to 1 if the species l is present in the position $\mathbf{r}$ or 0 otherwise, considering that only one species can occupy the position $\mathbf{r}$. So, with these definitions, all the information about the system is stored in $\psi(\mathbf{r},t)$. Consequently, we can express the average value of $\psi(\mathbf{r},t)$ as follows

$$\langle\psi(t)\rangle = \frac{1}{N^2}\sum_{\mathbf{r}}\psi(\mathbf{r},t), \tag{4.11}$$

where, $\langle\psi(t)\rangle$ is the order parameter of the system.

In the context of critical phenomena, the squared order parameter refers to the square of the magnitude of the order parameter. The order parameter is a measure of the degree of symmetry breaking in a system undergoing a phase transition, quantifying the difference between the ordered and disordered phases of the system. The square of the order parameter is performed to simplify calculations.

The definitions provided in equation (4.8) allow us to illustrate the behavior of $\psi(t)$ through the Figure 7, where each species is identified by a specific direction, represented by its associated phase, $e^{\frac{2\pi}{3}l}$, in the complex plane. The amplitude varies as the system evolves. As the parameter μ approaches the critical value μ_c, the intensity of the $\psi(t)$ increases significantly, accompanied by the emergence of a preferred direction for the phase of $\psi(t)$, this behavior is typical of phase transitions. In other words, as μ approaches μ_c, there is a gradual symmetry breaking in the system. This implies that one of the species fully occupies the lattice. Although, it is important to note that this process is inherently stochastic, and due to the non-hierarchical initial conditions defined in the system setup, it is not possible to predict which species will become dominant.

The Figure 8 illustrates the temporal dynamics of $|\langle\psi(t)\rangle|^2$, an expectation value that reflects the stability of the system. In regions far from the critical point μ_c, the plot indicates a stable, flat evolution, the value tends to remain around zero, indicating a well-defined phase with minimal fluctuations. However, as the system parameter μ approaches μ_c, $|\langle\psi(t)\rangle|^2$ shows pronounced fluctuations and an emerging phase transition signature.

When the system crosses the critical threshold, there is a clear stability in $|\langle\psi(t)\rangle|^2$, which indicates a new equilibrium state in another phase. This behavior confirms the phase transition. In summary, $\langle\psi(t)\rangle$ serves as an order parameter that describes the stability and phase dynamics of the system in three main regimes: stability far from μ_c, instability near mu_c, and a new equilibrium state after the transition.

4.3 Correlation Function Evaluation

The correlation function discussed in Section 3.4, commonly denoted as $G(\mathbf{r}-\mathbf{r}')$, serves as a measure of how the field at one point $\mathbf{r}$ in space relates to its value at another

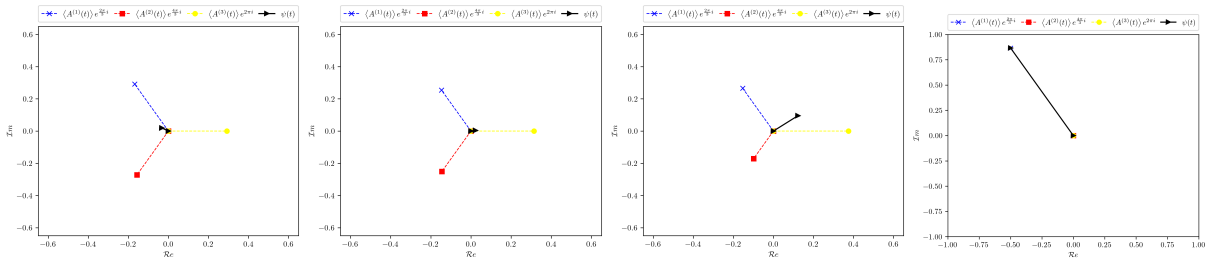

(a) $\mu << \mu_c$ (b) $\mu < \mu_c$ (c) $\mu \sim \mu_c$ (d) $\mu > \mu_c$

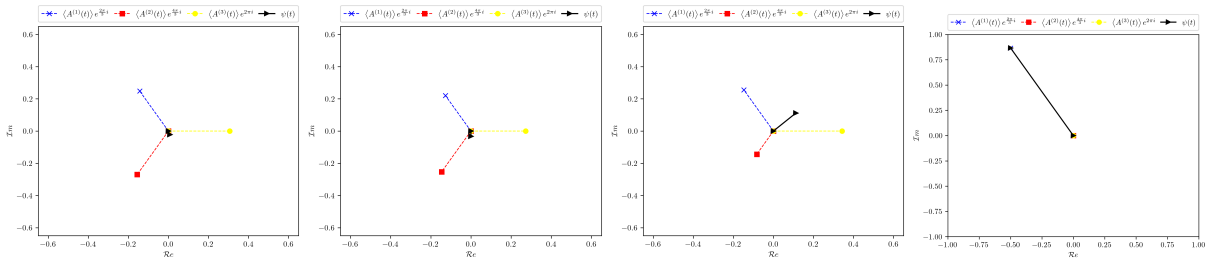

(e) $\mu << \mu_c$ (f) $\mu < \mu_c$ (g) $\mu \sim \mu_c$ (h) $\mu > \mu_c$

Figure 7 – Illustration of the variation in amplitude and direction of $\psi(t)$ for each generation step as μ approaches μ_c. The simulation parameters for each scenario are $\mu = 0.0100, \sigma = \lambda = 0.4950$ corresponding to panels **(a)**; $\mu = 0.7347, \sigma = \lambda = 0.1326$ for **(b)**; $\mu = 0.9617, \sigma = \lambda = 0.0192$ for **(c)**; $\mu = 0.9872, \sigma = \lambda = 0.0064$ for **(d)**; $\mu = 0.0100, \sigma = 0.6600, \lambda = 0.3300$ for **(e)**; $\mu = 0.7347, \sigma = 0.1769, \lambda = 0.0884$ for **(f)**; and $\mu = 0.9673, \sigma = 0.0218, \lambda = 0.0109$ for **(g)**, and $\mu = 0.9872, \sigma = 0.0085, \lambda = 0.0043$ for **(h)**. Source: Produced by the author.

point $\mathbf{r}'$. In a spatially homogeneous system, characterized by translational invariance, such as the system under consideration here, the correlation function is typically defined as an ensemble mean, and turns out to depend only on the relative distance between points, which simplifies its functional form, *i.e.*,

$$G(\mathbf{r} - \mathbf{r}') = \langle \psi^*(\mathbf{r}) \psi(\mathbf{r}') \rangle \,, \tag{4.12}$$

this function provides information about the spatial structure and extent of fluctuations in the field $\psi(\mathbf{r})$, where we omitted the time dependency for simplicity. It provides important details about the scale and range over which these fluctuations are correlated, and thus serves as a fundamental description of systems undergoing phase transitions or exhibiting critical phenomena.

In this context, we must analyze the correlation function in order to explore the fundamental and more general properties of our translationally invariant system. Translational symmetry of the correlation function in real space gives rise to a diagonal correlation function in Fourier space, thereby greatly simplifying the computational requirements for evaluating the correlation function. Performing a spatial Fourier transform allows the analysis of these symmetries in reciprocal space. In two dimensions, the Discrete

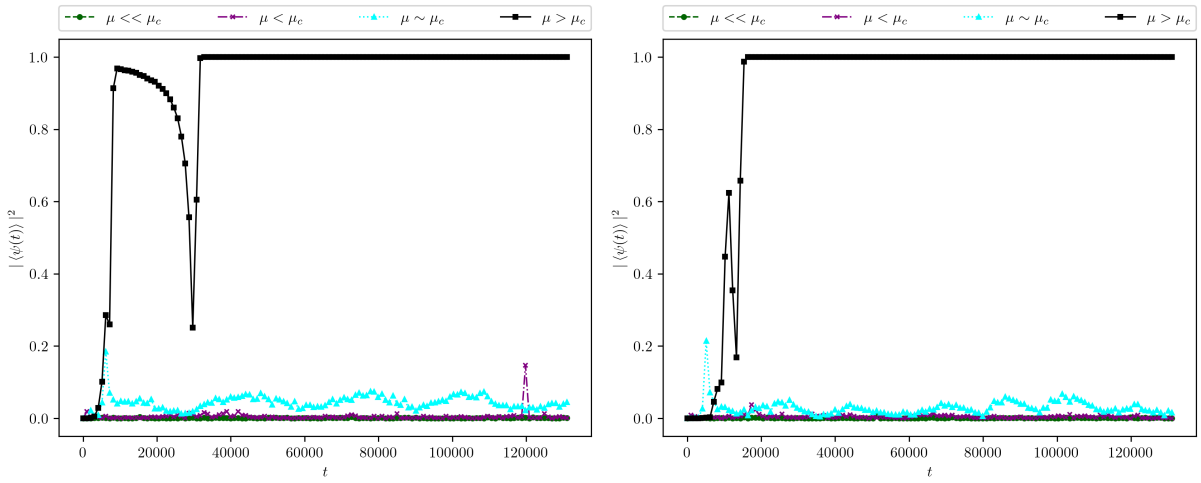

(a) (b)

Figure 8 – Illustration of the behavior of $|\langle\psi(t)\rangle|^2$ for each generation step as μ approaches μ_c. The parameters used in the simulation are: $\sigma = \lambda = \frac{\mu}{2}$ for (a), and $\lambda = \frac{\mu}{3}; \sigma = 2\lambda$ for (b). Source: Produced by the author.

Fourier Transform DFT is defined by,

$$F(\mathbf{k}) = \sum_{\mathbf{r}} f(\mathbf{r}) \cdot \exp\left(-i\,\mathbf{k}\cdot\mathbf{r}\right), \tag{4.13}$$

where the reciprocal lattice in Fourier space has spacing $\Delta k = \frac{2\pi}{N}$.

The DFT transforms a discrete signal $f(\mathbf{r})$ from the spatial domain into its wave-number domain representation $F(\mathbf{k})$. In the context of lattice systems with translational symmetry, the frequency domain is often represented within the first Brillouin zone. The Inverse Discrete Fourier Transform $IDFT$ is given by,

$$f(\mathbf{r}) = \frac{1}{N^2}\sum_{\mathbf{k}} F(\mathbf{k}) \cdot \exp\left(i\,\mathbf{r}\cdot\mathbf{k}\right), \tag{4.14}$$

and it serves to reconstruct the original signal $f(\mathbf{r})$ from its wave-number representation $F(\mathbf{k})$. Hence, we can now apply the Discrete Fourier transform to the field $\psi(\mathbf{r})$ and determine its corresponding representation in reciprocal space, denoted as $\Psi(\mathbf{k})$,

$$\Psi(\mathbf{k}) = \sum_{\mathbf{r}} \psi(\mathbf{r}) \cdot \exp\left(-i\,\mathbf{k}\cdot\mathbf{r}\right), \tag{4.15}$$

and the Inverse Discrete Fourier Transform,

$$\psi(\mathbf{r}) = \frac{1}{N^2}\sum_{\mathbf{k}} \Psi(\mathbf{k}) \cdot \exp\left(i\,\mathbf{r}\cdot\mathbf{k}\right). \tag{4.16}$$

Therefore, after the calculation of $\Psi(\mathbf{k})$, we can calculate the correlation function of our

system, which is given by $\langle \Psi^*(\mathbf{k})\Psi(\mathbf{k}')\rangle$, thus

$$G(\mathbf{k},\mathbf{k}') = \langle \Psi^*(\mathbf{k})\Psi(\mathbf{k}')\rangle\,, \tag{4.17}$$

$$= \sum_{\mathbf{r}}\sum_{\mathbf{r}'} \exp\left(-i\,\mathbf{k}\cdot\mathbf{r} + i\,\mathbf{k}'\cdot\mathbf{r}'\right)\,\langle \psi^*(\mathbf{r})\psi(\mathbf{r}')\rangle\,, \tag{4.18}$$

$$= \sum_{\mathbf{r}}\sum_{\mathbf{r}'} \exp\left(-i\,\mathbf{k}\cdot\mathbf{r} + i\,\mathbf{k}'\cdot\mathbf{r}'\right) G(\mathbf{r}-\mathbf{r}'), \tag{4.19}$$

substituting $\mathbf{r} = \mathbf{R} + \mathbf{r}'$,

$$G(\mathbf{k},\mathbf{k}') = \sum_{\mathbf{r}'}\sum_{\mathbf{R}} \exp\left(-i\,\mathbf{k}\cdot(\mathbf{R}+\mathbf{r}') + i\,\mathbf{k}'\cdot\mathbf{r}'\right) G(\mathbf{R}), \tag{4.20}$$

$$= \sum_{\mathbf{r}'} \exp\left[-i\,\mathbf{r}'\cdot(\mathbf{k}-\mathbf{k}')\right] \sum_{\mathbf{R}} \exp\left(-i\,\mathbf{k}\cdot\mathbf{R}\right) G(\mathbf{R}), \tag{4.21}$$

$$= N^2\delta_{\mathbf{k},\mathbf{k}'} \sum_{\mathbf{R}} \exp\left(-i\,\mathbf{k}\cdot\mathbf{R}\right) G(\mathbf{R}), \tag{4.22}$$

$$= \delta_{\mathbf{k},\mathbf{k}'} N^2 g(\mathbf{k}), \tag{4.23}$$

where $\delta_{\mathbf{k},\mathbf{k}'}$ is the Kronecker delta symbol, and

$$g(\mathbf{k}) = \sum_{\mathbf{R}} \exp\left(-i\,\mathbf{k}\cdot\mathbf{R}\right) G(\mathbf{R}). \tag{4.24}$$

Hence, through equation (4.24), we can obtain the correlation function of our system.

In the Figure 9, we observe that the greater the distance from μ to μ_c, the more delocalized becomes $g(\mathbf{k})$, while as μ approaches μ_c, the distribution of $g(\mathbf{k})$ becomes concentrated around $\mathbf{k} = 0$. The width k_c of $g(\mathbf{k})$ can be used to define the system's correlation length

$$\xi = \frac{2\pi}{k_c}. \tag{4.25}$$

A highly concentrated $g(\mathbf{k})$ around $\mathbf{k} = 0$ indicates the divergence of ξ and the presence of long-range correlations which are typical at the onset of a phase-transition.

This characterizes the point at which the symmetry of the system breaks, leading to a transition from diversity to uniformity. In real space, this transition is typified by one species filling all sites in the lattice.

The correlation length provides essential information about how physical systems behave near critical points. It represents the characteristic distance over which fluctuations in a system are correlated and thus serves as a measure of the behavior of the system. For example, in the study of phase transitions, when a material undergoes a phase transition, such as from a solid to a liquid, the correlation length can reveal how far the influence of fluctuations in the order of the material extends. In the context of magnetic materials, the correlation length can help to understand how the orientation of the atomic magnetic moments evolves as the material approaches its Curie temperature. Thus, the correlation length provides a quantitative measure of the range of correlations between elements in a system.

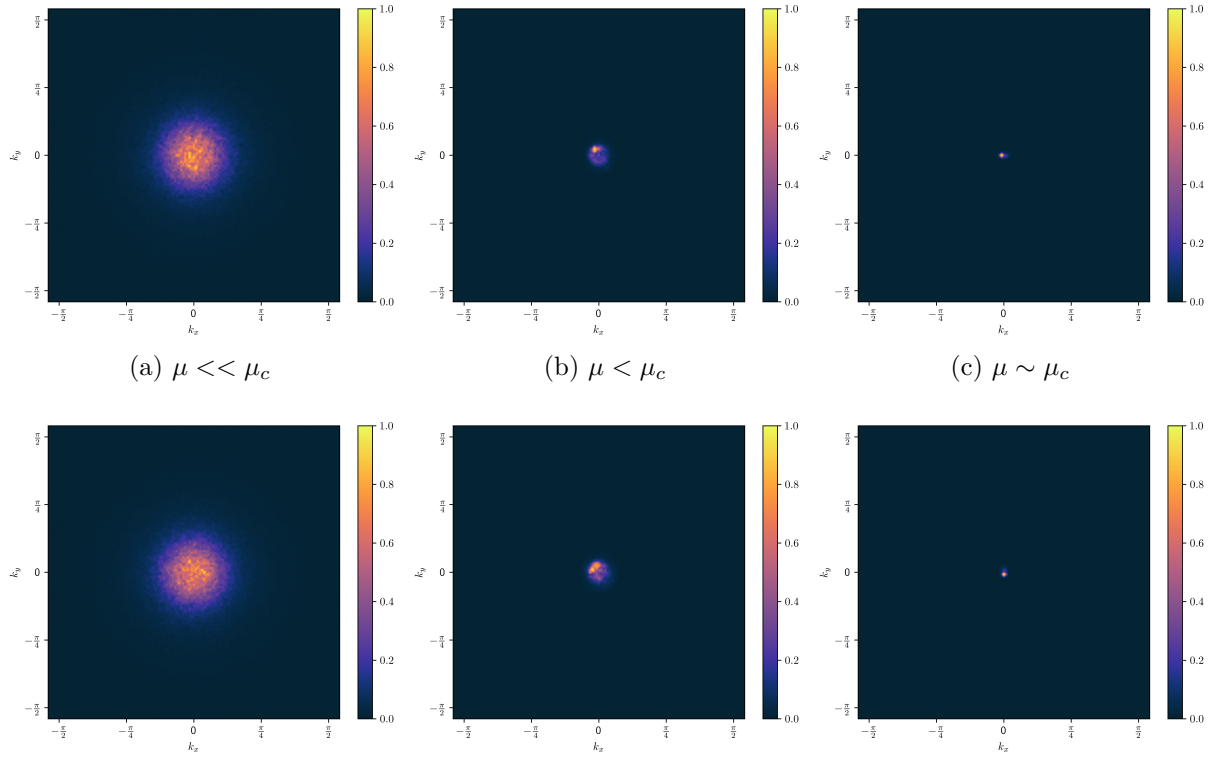

(a) $\mu << \mu_c$ (b) $\mu < \mu_c$ (c) $\mu \sim \mu_c$

(d) $\mu << \mu_c$ (e) $\mu < \mu_c$ (f) $\mu \sim \mu_c$

Figure 9 – Density Profile of correlation function $g(\mathbf{k})$ in reciprocal space at different distances to the critical point. The amplitude of $g(\mathbf{k})$ is normalized, and the color intensity indicates the magnitude of the correlation function. **(a)** and **(d)** As the system is distant from the critical point, the correlation function $g(\mathbf{k})$ manifests a greater dispersion and evolves along a smoother profile. **(b)** and **(e)** As the critical transition zone is approached, the correlation function $g(\mathbf{k})$ undergoes a compression in its spatial domain, combined with an intensification of its correlation magnitude. **(c)** and **(f)** Near the critical transition boundary, the distribution function $g(\mathbf{k})$ localizes more strongly around $\mathbf{k} = 0$, resulting in a significant increase in the magnitude of the correlation function. The parameters used in the simulation are: $\mu = 0.0100, \sigma = \lambda = 0.4950$ (a), $\mu = 0.7347, \sigma = \lambda = 0.1326$ (b), $\mu = 0.9617, \sigma = \lambda = 0.0192$ (c), $\mu = 0.0100, \sigma = 0.6600, \lambda = 0.3300$ (d), $\mu = 0.7347, \sigma = 0.1769, \lambda = 0.0884$ (e), and $\mu = 0.9617, \sigma = 0.0255, \lambda = 0.0128$ (f). Source: Produced by the author.

In Figure 10, the distribution of the blue species is represented by an emerging pattern of spirals that progressively expand in size. This expansion continues until the spirals extend throughout the entire lattice, leading to the complete filling of all sites. This visual representation captures the dynamic process of spatial pattern evolution and illustrates how localized structures gradually expand to dominate the entire system.

In the vicinity of a critical point, exemplified by scenarios like the boiling point in the context of liquids or the Curie temperature for ferromagnetic materials, a notable phenomenon emerges: the correlation length exhibits a tendency to diverge. In practical terms, this signifies that fluctuations within the system undergo a remarkable transformation,

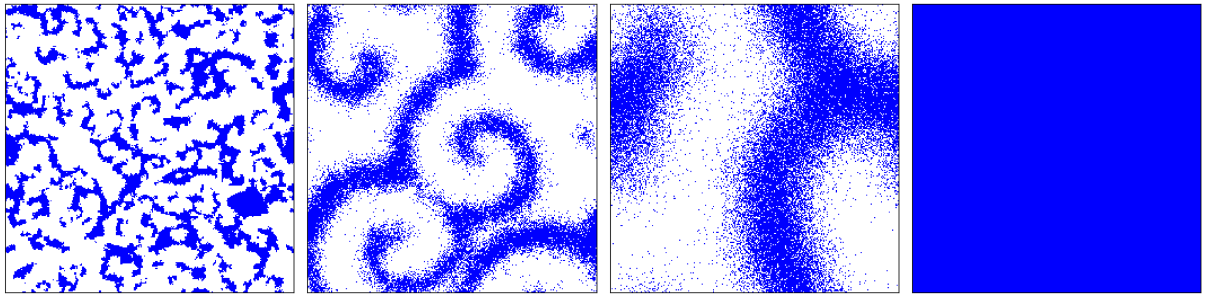

(a) $\mu << \mu_c$ (b) $\mu < \mu_c$ (c) $\mu \sim \mu_c$ (d) $\mu > \mu_c$

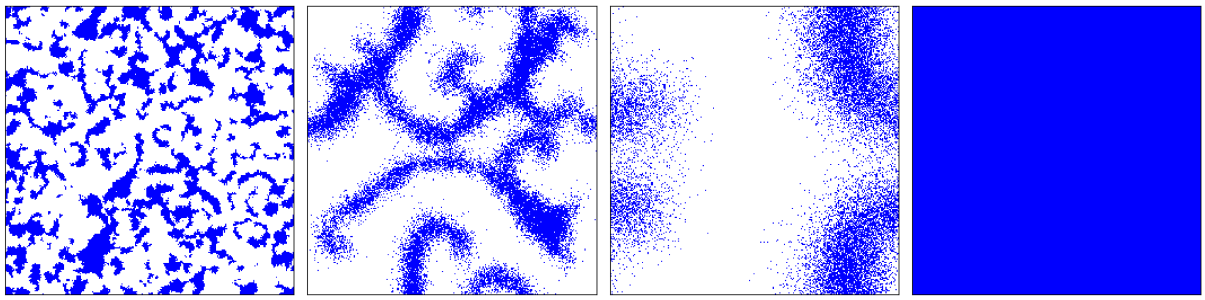

(e) $\mu << \mu_c$ (f) $\mu < \mu_c$ (g) $\mu \sim \mu_c$ (h) $\mu > \mu_c$

Figure 10 – Formation of spatial patterns for different ranges of μ. Formation of clusters, complex spirals and plane wave fronts, and fulfilling of the lattice in real space. **(a)** and **(e)** Formation of Clustered Patterns: Characterizes the emergent behavior of localized aggregations. **(b)** and **(f)** Emergence of Complex Spirals: Describes the emergence of complex spiral configurations in the system. **(c)** and **(g)** Wavefront-like Spatial Patterning: Describes a flat, advancing configuration similar to a wavefront. **(d)** and **(h)** Total filling by a single species when reaching μ critical: Denotes a state where the entire domain is occupied by a single species when the parameter μ reaches its critical value, μ_c. The simulation parameters for each scenario are $\mu = 0.0100, \sigma = \lambda = 0.4950$ corresponding to panels (a); $\mu = 0.7347, \sigma = \lambda = 0.1326$ for (b); $\mu = 0.9617, \sigma = \lambda = 0.0192$ for (c); $\mu = 0.9872, \sigma = \lambda = 0.0064$ for (d); $\mu = 0.0100, \sigma = 0.6600, \lambda = 0.3300$ for (e); $\mu = 0.7347, \sigma = 0.1769, \lambda = 0.0884$ for (f); and $\mu = 0.9673, \sigma = 0.0218, \lambda = 0.0109$ for (g), and $\mu = 0.9872, \sigma = 0.0085, \lambda = 0.0043$ for (h). Source: Produced by the author.

becoming intrinsically tied to one another over progressively greater spatial extents [2].

The singular behavior of the correlation length ξ as a physical system approaches a critical point [40], such as a phase transition, means that the correlation length tends to grow significantly, and approaches infinity. This phenomenon is a principal indicator that the system is approaching a phase transition, such as the solidification of a liquid, the magnetization of a ferromagnetic material or the condensation of a gas. The correlation length divergence is related to other important concepts such as critical exponents and universality. As ξ diverges, fluctuations in different parts of the system become strongly correlated, leading to universal critical properties that do not depend on the microscopic details of the system, and their divergence behavior is related to the critical exponent ν as

described in equation (3.10), and the distance to the critical point by the relation [40],

$$\xi \sim |\mu - \mu_c|^{-\nu}. \tag{4.26}$$

The relation (4.26) states that as the control parameter μ approaches the critical value μ_c, the correlation length ξ diverges following a power-law behavior. The exponent ν indicates the rate at which this divergence occurs. Therefore, it tells us how sensitive the correlation length is to changes in the control parameter near the critical point. This relation is fundamental to understand the behavior of systems undergoing phase transitions and is a fundamental concept in the study of critical phenomena.

4.4 Scaling Hypothesis

The scaling hypothesis states that near the critical point, $\mu \to \mu_c$, the correlation length ξ emerges as the only characteristic length scale of a system [55]. This is supported by our numerical experiments and theory [2, 55] suggests that ξ tends to infinity at the critical threshold, implying the absence of any characteristic length at the critical point and, consequently, the scale invariance of the system. Scale invariance implies that if a portion of the system is magnified to the scale of a large portion of the system, there is no observable difference between the magnified portion and the original system, thus indicating self-similarity across scales [55]. This concept is captured quantitatively by the statement that all thermodynamic functions are homogeneous near the critical point [55].

As discussed in section 3.3, the homogeneity assumption implies restrictions on the properties of a function. If any function satisfies an equation of the form (3.14) or equivalently (3.17), then it is classified as a homogeneous equation [2]. By considering that this is the case for our correlation function near the critical point, it follows that,

$$G(\alpha^a \mathbf{r}, \alpha^b \xi) = \alpha G(\mathbf{r}, \xi), \tag{4.27}$$

where α^a and α^b are scaling factors, with $\alpha > 0$. Let us consider now the special case

$$\alpha = \xi^{-\frac{1}{b}}. \tag{4.28}$$

By substituting (4.28) in (4.27), we obtain:

$$G(\xi^{-\frac{a}{b}} \mathbf{r}, 1) = \xi^{-\frac{1}{b}} G(\mathbf{r}, \xi). \tag{4.29}$$

In a similar way to (3.16), where $F(y) \equiv f(y, 1)$, we can rewrite (4.29) as:

$$G(\mathbf{r}, \xi) = \xi^{\frac{1}{b}} \bar{G}(\xi^{-\frac{a}{b}} \mathbf{r}). \tag{4.30}$$

Thus, the correlation function G can be expressed both in the forms of (4.27) and (4.29), which correspond to the forms of (3.14) and (3.17), respectively. Consequently, $G(\mathbf{r}, \xi)$

is a homogeneous function, and so is $g(\mathbf{k}, \xi)$. We are interested in the asymptotic form of the correlation function (4.30), where ξ becomes the only relevant length. Thus, the asymptotic behavior must be given by [58, 67]

$$G(\mathbf{r}, \xi) \sim \mathbf{r}^{-u} \bar{G}(\frac{\mathbf{r}}{\xi}), \tag{4.31}$$

therefore we must have $b = -\frac{1}{u}$, $a = b$, in agreement with (3.13).

In this thesis, we consider the approach to the critical point through two different paths: $\sigma = \lambda = \frac{\mu}{2}$ and $\lambda = \frac{\mu}{3}; \sigma = 2\lambda$. Our objective is to numerically demonstrate that the correlation function is indeed homogeneous and that the results for the critical exponents do not depend on the path approaching the critical point, *i.e.*, the critical behavior is the same. For each value of the parameter μ for each approaching path we numerically obtained a plot of the correlation function, shown in Figure 11 of chapter 5, where each curve turns out to have a different correlation length.

In order to obtain the critical exponent ν, described by the equation (4.26), it is more convenient to scale the correlation function in equation (4.31) relative to the correlation length ξ in reciprocal space. Scaling these curves to collapse into a single functional form allows a precise determination of both the critical exponents and thus potentially provide information about the associated universality class of the system. Consequently, it is necessary to consider the simultaneous scaling of both variables in $g(\mathbf{k}, \rho)$ according to (4.27), where $\rho = |\mu - \mu_c|$. This parameter ρ encapsulates the extent to which the system deviates from its critical point, thereby providing a metric for assessing its critical behavior.

In the vicinity of the critical point, under the conditions of $k \ll \frac{2\pi}{\Delta r}$, and $\xi \gg \Delta r$, the equation (4.24), becomes

$$g(\mathbf{k}, \rho) \simeq \frac{1}{(\Delta r)^d} \int \mathrm{d}^d r \exp(-i\mathbf{k} \cdot \mathbf{r})\, G(\mathbf{r}, \xi). \tag{4.32}$$

In this context, the function $G(\mathbf{r}, \xi)$ is given by the equation (4.31), which takes the form described in the equation (3.17). The correlation length ξ diverges as the system approaches the critical point, this behavior is captured by

$$\xi \sim \rho^{-\nu}, \tag{4.33}$$

then, by substituting the expressions for $G(\mathbf{r}, \xi)$ from equation (4.31), and ξ from equation (4.33) into equation (4.32) for $g(\mathbf{k}, \rho)$, we obtain the following result:

$$g(\mathbf{k}, \rho) = \int \mathrm{d}^d r \, \exp(-i\mathbf{k} \cdot \mathbf{r}) \mathbf{r}^{-u} \bar{G} \left(\frac{\mathbf{r}}{\xi} \right), \tag{4.34}$$

where we assume equality, since any prefactor can be incorporated into the definition of $\bar{G}(\mathbf{r})$. We can make a change of variables by taking $\mathbf{r} \to \xi \mathbf{r}$, which implies $\mathrm{d}^d r \to \xi^d \mathrm{d}^d r$

and $\mathbf{r}^{-u} = \xi^{-u}\mathbf{r}^{-u}$, thus we obtain

$$g(\mathbf{k},\rho) = \xi^{d-u}\int \mathrm{d}^d r\, \exp(-i\xi\mathbf{k}\cdot\mathbf{r})\mathbf{r}^{-u}\bar{G}(\mathbf{r}), \tag{4.35}$$

$$= \xi^{d-u}\bar{g}\left(\xi\mathbf{k}\right), \tag{4.36}$$

$$= \rho^{-\nu(d-u)}\bar{g}(\rho^{-\nu}\mathbf{k}), \tag{4.37}$$

we simplified the notation in a manner analogous to that demonstrated in the equation (3.16), so that the correlation function in reciprocal space is expressed by $\bar{g}(\rho^{-\nu}\mathbf{k}) = g(\rho^{-\nu}\mathbf{k}, 1)$.

On the other hand, thermodynamic compressibility, as defined in the equation (3.6), is commonly associated with the magnitude of fluctuations in particle density [68]. Compressibility essentially quantifies how much the density of a system varies in response to changes in pressure, reflecting the capacity of the system to accommodate such fluctuations. While our system does not directly provide this physical quantity, we can establish a relation to it through the correlation function in reciprocal space, as indicated by the relation [2],

$$K = \int \mathrm{d}^d r G(\mathbf{r}) \tag{4.38}$$

$$= \rho^{-\gamma}, \tag{4.39}$$

with ρ as a control parameter, and

$$K = \int \mathrm{d}^d r G(\mathbf{r}) \tag{4.40}$$

$$= \int \mathrm{d}^d r \exp(-i\mathbf{k}\cdot\mathbf{r})G(\mathbf{r}) \tag{4.41}$$

$$= g(\mathbf{k}=0). \tag{4.42}$$

Hence, by combining the results from Equations (4.39) and (4.42), we obtain

$$g(\mathbf{k}=0) = \rho^{-\gamma}. \tag{4.43}$$

Consequently, the exponent γ is related to the correlation function at $\mathbf{k}=0$. Therefore, combining the result from equation (4.37) and (4.43) at $\mathbf{k}=0$, we obtain the following scaling relation:

$$\rho^{-\nu(d-u)} = \rho^{-\gamma}, \tag{4.44}$$

thus, we conclude the scaling relation

$$\gamma = \nu(d-u). \tag{4.45}$$

By substituting the result from Equation (4.45) into the outcome of Equation (4.37), we obtain the following expression [58, 67],

$$g(\mathbf{k},\rho) = \rho^{\gamma}\bar{g}(\rho^{\nu}\mathbf{k}). \tag{4.46}$$

Hence, we conclude that near the critical point, the correlation function in Fourier space also takes the form described by equation (3.17), *i.e.*, it is also a homogeneous function. For our system, the behavior described in equation (4.46) will be demonstrated in chapter 5, where it is shown that all curves in the vicinity of the critical point can be made to coincide with a single unified curve by applying proper scaling transformations. We demonstrate that such scale invariance remains true even if the critical point is approached through different paths. The successful collapse of these curves allows a direct calculation of the critical exponents ν and γ. Additionally, it enables us to indirectly determine the value of η through equation (3.26). Therefore, as the system approaches the critical point, symbolized by $\rho \to 0$, the correlation length ξ diverges, following the power law $\xi \sim \rho^{-\nu}$, with $\nu > 0$. Such exponents characterize the critical behavior of this system.

5 Critical Analysis

5.1 Self-Similarity

This chapter presents the results of our study on critical phenomena in the RPS model. We used numerical experiments and computational simulations to investigate the complex dynamics and characteristics of the RPS model near the critical point. Our findings are important for validating theoretical models and enhance our understanding of systems at the threshold of criticality in models governed by fundamental cyclic interactions [13].

In research on complex biological systems, the use of critical phenomena theory from statistical physics provides a novel methodological framework [2, 40, 58]. This theory is relevant for understanding phase transitions and scaling in physical systems and provides a unique perspective for examining the complex dynamics of ecological interactions [13]. The RPS model, which is simple yet effective in capturing competitive interactions among species [17, 18, 27], serves as a key example to underscore its relevance. The integration of critical phenomena principles with the RPS model provides a better comprehension of critical behaviors in ecosystems. This underlines the potential of the RPS model to unravel the complexity of ecological dynamics.

The methodologies employed in this research combine theoretical approaches and computational techniques chosen for their robustness and relevance to our investigation of critical phenomena and extraction of critical exponents. Our numerical approach has sufficient accuracy, while enabling simulation of system behavior in the critical regime.

We conducted numerical experiments and built our own data sets after reviewing the relevant literature [17, 18, 25, 27, 34]. Data collection was performed through computational simulations using codes designed by the author, guided by the RPS model. These simulations enabled the estimation of the critical movement, μ_c, and the critical exponents γ, ν, and η, as well as the study of system dynamics near the transition region.

Our findings suggest that below the critical movement threshold, the system develops intricate patterns such as species clustering, indicative of diversity (or biodiversity), as shown in Figures 10a and 10e. This observation is in agreement with what is reported in literature [27]. Moreover, we observed a notable increase in the size of the spiral pattern arms as the system approaches critical movement [27, 34], as shown in Figure 10c and 10g. In particular, the structure of these spirals extends beyond the lattice dimensions, as shown in Figure 10d and 10h, confirmed by [34]. Consequently, the diverse patterns dissipate and the system transitions to uniformity. In this phase, the dominance of a single species occurs, resulting in the extinction of the other two. Fourier Transforms were

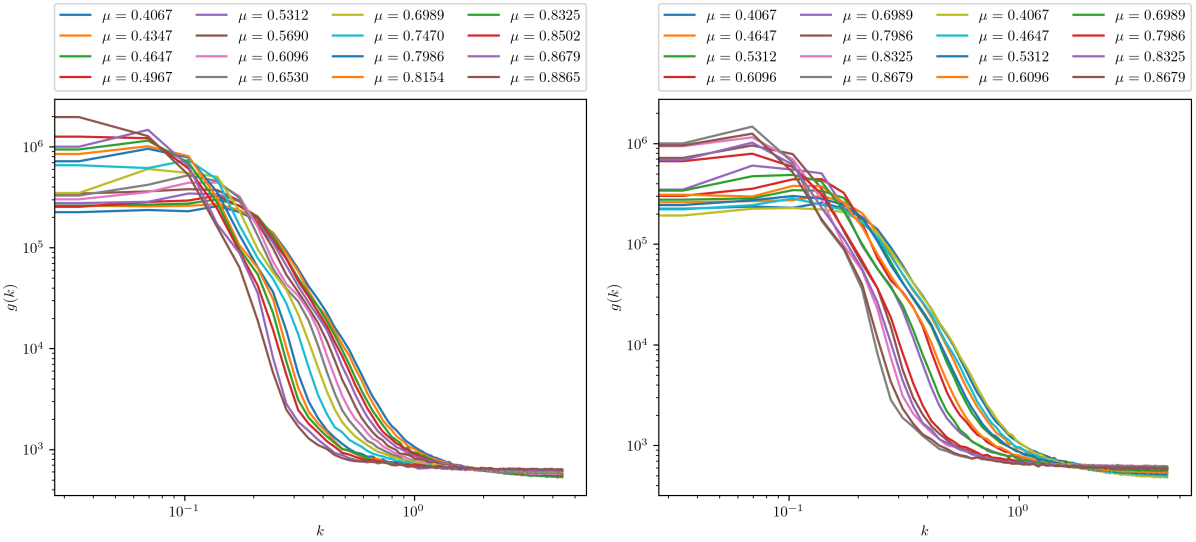

(a) (b)

Figure 11 – Radial profile of the correlation function $g(\mathbf{k})$ in reciprocal space for varying values of the control parameter μ, following angular averaging. Simulation parameters are set as: $\sigma = \lambda = \frac{\mu}{2}$ for (a), and $\lambda = \frac{\mu}{3}; \sigma = 2\lambda$ for (b). Source: Produced by the author.

performed to explore spatial fluctuations and correlations within the system, as shown in equation (4.24) and illustrated in Figure (9), thus providing a significant contribution to our analytical framework.

Angular averaging was performed since our function has rotational symmetry on average. By integrating the function in a disc, the numerical noise is attenuated, thus leaving a function that depends only on the radial distance in Fourier space, hence $g(\mathbf{k}) \to g(k)$, where $k = |\mathbf{k}|$, simplifying the analysis. The correlation functions $g(\mathbf{k})$, shown in Figure 9, can also be analyzed through the radial profiles shown in Figure 11. Such plots must be subjected to scaling transformations as discussed in Section 4.4 in order to reveal the self-similar structure of for such plots.

In the Figure 11, each curve corresponds to a different correlation length. According to the hypothesis of homogeneity [2, 19] of the correlation function, it should be possible to find a general homogeneous function capable of describing all curves in the vicinity of the critical point, thus providing a unified representation of the system behavior in this region.

Our research aims to validate the previously mentioned hypothesis. By examining the different correlation lengths for each curve shown in Figure 11 and using the concept of homogeneity in the correlation function. We aim to identify a general homogeneous function that describes all curves in the vicinity of the critical point, thus allowing a unified characterization of the system behavior in this region. This approach is supported

by the discussion in chapter 4, where we expect the system dynamics to be consistent with the formulation presented in equation (4.46), thus establishing a direct correspondence between our empirical analysis and the theory.

The concept of self-similarity and scale invariance is at the core of this phenomenon. As the system approaches the critical point, the correlation function, as expressed in the equation (4.46), becomes self-similar, *i.e.*, invariant under scale transformations. This implies that the structure of the system exhibits repeating patterns across different scales of observation, revealing the presence of universal features that persist regardless of the scale of measurement. Figure 11 illustrates this self-similarity property, showing how radial correlation profiles maintain similar patterns at different distances from the critical point. This observation underscores the importance of self-similarity in understanding and characterizing critical phenomena in physical systems.

Near the critical point, the curves exhibit a distinctive behavior as the system approaches this singular region. This behavior is characterized by the divergence of the correlation length according to power laws [2, 19, 58]. Such divergence signifies the emergence of long-range correlations and critical behavior, indicating the imminent transition of the system to a critical state [40].

Our work draws important parallels between the studied system and condensed matter systems [2, 19, 40, 58, 60, 69]. Although there may be differences, the RPS model can exhibit critical signatures similar to those observed in well-described physical systems. This underlines the potential of the model for the demonstration of phenomena which are well established in the literature. The critical phenomena theory approach to the RPS model has not been explored within the current scope of our understanding. This unconventional approach provides fresh perspective on complex systems, revealing critical behaviors that have not yet been explored or documented in the existing literature.

5.2 Scaling Behavior

In this section, we expose a method for demonstrating the homogeneity for the two-point correlation function $g(k, \rho)$ which is depicted in Figure 11 for different distances from the critical point $\rho_i = |\mu_i - \mu_c|$ which for small wavelengths can be expressed according to,

$$g(k, \rho) = \rho^{\gamma} \bar{g}(\rho^{\nu} k). \tag{5.1}$$

This equation encapsulates the essence of how the correlation function scales with the parameter ρ, characterized by the critical exponents γ and ν, and a scaling function $\bar{g}$. Indeed, by considering a reference distance ρ_0, a correlation function $g(k, \rho_i)$ associated to any distance ρ_i can be made to coincide with $g(k, \rho_0)$ through a scale transformation, *i.e.*,

$$\left(\frac{\rho_0}{\rho_i}\right)^{\gamma} g\left(\left(\frac{\rho_0}{\rho_i}\right)^{\nu} k, \rho_i\right) = g(k, \rho_0), \tag{5.2}$$

for any ρ_i according to (5.1).

The objective is to establish a quantitative measure, specifically a mean square error E, which reflects the deviation between the values of the correlation function at different $g(k, \rho_i)$ and a selected reference state $g(k, \rho_0)$.

The calculation of E involves determining the squared differences between the logarithmically transformed, scaled correlation function at different ρ_i and the logarithm of the correlation function at the reference state ρ_0. This procedure is repeated for n distinct ρ_i, and the results are averaged to procure the mean squared error,

$$E = \frac{1}{n} \sum_{i=1}^{n} \sum_{k} \left(\log \left[\left(\frac{\rho_0}{\rho_i} \right)^{\gamma} g \left(\left(\frac{\rho_0}{\rho_i} \right)^{\nu} k, \rho_i \right) + 1 \right] - \log(g(k, \rho_0) + 1) \right)^2, \tag{5.3}$$

where ρ_0 and ρ_i represent the deviations from the critical movement μ_c for the reference and the i^{th} curve, respectively, and n denotes the total number of considered curves in the vicinity of the critical point. The logarithm allows for the comparison between different scales in the error function. We modify the logarithm arguments by adding a unitary term to avoid any divergence due to a vanishing logarithm argument. This adjustment ensures that the logarithm remains well-defined over the entire range of $g(k, \rho)$ values. Eq. (5.3), is thus chosen by us as a metric for quantifying the degree of disagreement between rescaled correlation functions across different parameters and the reference correlation function.

To minimize the mean squared error described by the equation (5.3), an exhaustive exploration of the parameter space is performed, aka brute force, for the parameters μ_c, γ, and ν, in order to identify the parameter set that minimizes E.

As opposed to gradient method, the exhaustive search strategy verify every possible combination within the solution space, assuming that it is possible to fully explore this space within reasonable time and resource constraints. This thorough evaluation ensures the identification of the absolute best solution, which is critical for noisy data which is our case.

Although in the Figure 12 the data appears smooth, a more detailed analysis reveals the existence of small fluctuations. We can see in the figures that around the minimum values the error function is almost flat, which means that in these regions the gradients of the noise become too pronounced, thus making the use of gradient methods inviable.

The limitation of gradient-based methods can be avoided by using Simulated Annealing [70], a technique that provides a stochastic means of approaching global minimization, potentially solving the limitations of local minima that gradient methods may encounter. However, in a system with only three variables, the brute force method becomes viable and represents the most accurate approach. By exhaustively searching through all possible solutions, the brute force method guarantees the identification of the optimal solution.

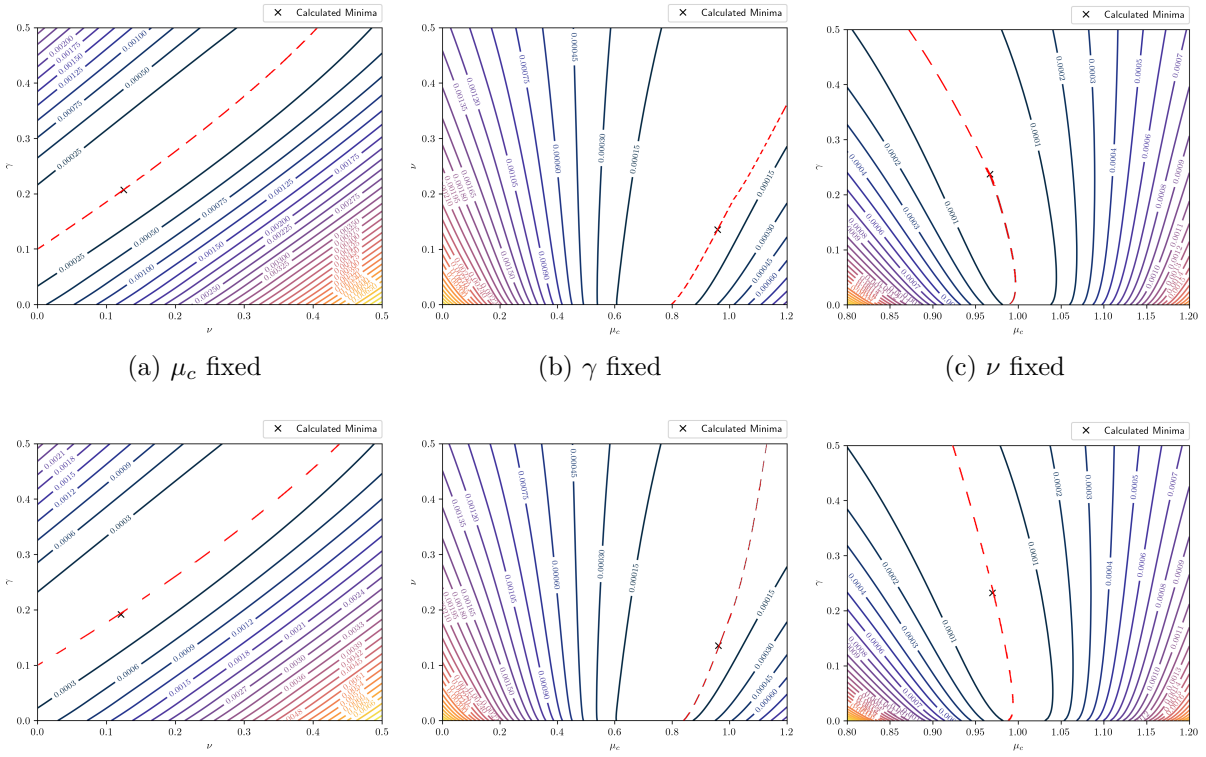

(a) μ_c fixed (b) γ fixed (c) ν fixed

(d) μ_c fixed (e) γ fixed (f) ν fixed

Figure 12 – Contour maps of E for fixed parameters: Each plot showcases variations against two changing parameters (μ_c, γ, ν), illustrating the intricate relationship between parameter adjustments and error minimization. **(a)** and **(d)** μ_c fixed: E variation with γ and ν, for fixed μ_c. **(b)** and **(e)** γ fixed: Contour map of E versus μ_c and ν, with constant γ. **(c)** and **(f)** ν fixed: E response to γ and μ_c changes, with ν constant. The points marked with an "$\times$" on the picture represent the minimum error found by the exhaustive search for our system, detailed in Table 2. The simulation parameters are set as follows: $\sigma = \lambda = \frac{\mu}{2}$ for figures (a), (b), and (c). For figures (d) and (e), the parameters are adjusted to $\lambda = \frac{\mu}{3}$ and $\sigma = 2\lambda$. Source: Produced by the author.

The contour plots shown in Figure 12 display mean square error, landscapes for fixed parameters γ, μ_c, and ν, respectively. It illustrates the variation of E over the parameter space. Mapping contours of equal E values help us to isolate promising regions of the parameter space for deeper analysis, thereby improving the optimization process in the presence of noise.

By identifying the optimal set of parameters (μ_c, γ, ν), we achieved the smallest mean square error as delineated by equation (5.3). Following this minimization, the critical point μ_c, along with the critical exponents γ and ν, were obtained and are detailed in table 2. By applying the scale transformations (5.2) to all curves in Figure 11 according to the parameters in the table 2, were finally able to demonstrate the self-similarity near the critical point, as shown in Figure 13. This confirms the homogeneity of the two-point correlation function. Additionally, by applying the hyperscaling relation described in

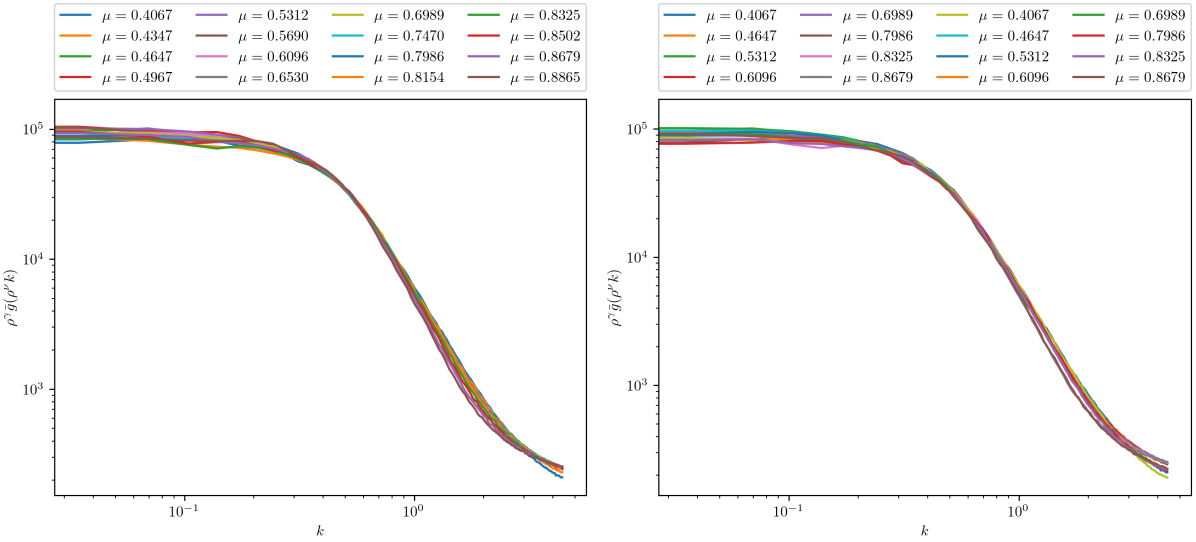

(a) (b)

Figure 13 – **(a)** and **(b)** Scaling of the correlation function $g(k)$ in the reciprocal space for different values of the scaling parameter ρ, after angular averaging. The parameters used in the simulation are: $\sigma = \lambda = \frac{\mu}{2}$ (a), and $\lambda = \frac{\mu}{3}; \sigma = 2\lambda$ (b).

equation (3.26), the critical exponent η was computed, with values presented in table 2.

The concept of self-similarity, here observed in the context of a homogeneous correlation functions, is a fundamental aspect of critical phenomena. It denotes the intrinsic property of a system or pattern to be invariant under scaling transformations. This property is not purely of mathematical interest, but serves as the foundation for the derivation of scaling laws, which are essential for predicting the behavior of systems at different scales.

The importance of self-similarity in critical systems is exemplified by the universal nature of critical exponents. These exponents, observable in diverse systems such as the magnetic domains in ferromagnetic to the intricate lattices in disordered media, describe how physical quantities such as magnetization and correlation lengths diverge as the system approaches criticality [2, 19]. Theoretical milestones, notably Kadanoff's scaling hypothesis [1] and Wilson's renormalization group theory [4], provide the foundation for understanding the self-similarity of these phenomena. Their collective findings have revealed the nature of the underlying symmetries at critical points, thus allowing the formulation of predictions that are consistent with empirical evidence in both experimental and real-world systems. In this thesis, it is important to clarify that the self-similarity within this system is not derived from first principles as for example through renormalization group theory. In thesis, we are merely reporting the discovery of emergent self-similar structures in the RPS model. A comprehensive explanation and exploration of this phenomenon seems to be a significant area of interest that requires further investigation. Consequently, a more fundamental analysis of origins of this critical behavior is left as a suggestion for future research efforts.

Table 2 – Critical Exponents Evaluation.

μ_c	ν	γ	η
0.9662	0.1374	0.235	0.29

Source: Produced by Author.

5.3 Critical Exponents

As described in Chapter 3, critical exponents are essential for understanding phase transitions and critical phenomena by revealing how thermodynamic quantities behave as the critical point is approached. The fundamental relationship between these exponents and universality classes was described by Fisher [3, 5], establishing a theoretical framework that has been applied extensively in the field. The exponents, such as α for specific heat and β for magnetization, have been instrumental in explaining the singular behavior of systems on the threshold of criticality. Stanley [2], building on Weiss's [71] initial findings, provided a thorough analysis of the magnetization in ferromagnetic systems, thereby improving the understanding of phase transitions.

In addition, exponents such as γ, ν, and δ encapsulate the nuances of susceptibility, correlation length, and order parameter response, respectively, as discussed in the same chapter. Onsager's [72] exact solutions for the two-dimensional Ising model provided a quantitative prediction for γ, and both Kadanoff's block-spin argument [1] and Widom's scaling hypothesis [73] were central to developing the conceptual framework for understanding ν and δ. These theoretical developments, coupled with the hyperscaling relations involving system dimensionality [5, 73], are essential to the scaling theory that characterizes the critical region. In addition, the introduction of the dynamical critical exponent z by Hohenberg and Halperin [29] further refined the classification of dynamical systems into universality classes, reflecting the intricate relationship between dynamic and static critical phenomena.

As a result of our research, we determined the critical point μ_c and the critical exponents γ and ν using the error minimization method. Additionally, considering the hyperscaling relations, we computed the critical exponent η. The proximity of the critical movement parameter μ_c to unity, as shown in Table 2, leads us to believe that the actual value of the critical movement parameter is indeed equal to 1. In addition, we demonstrated that the critical point is the same whatever the path taken to this critical limit, as demonstrated by our analyses. The data shown in Table 2 are obtained from the average values found for (μ_c, γ, ν) at the variation of the parameters with the following proportions: $\sigma = \lambda = \frac{\mu}{2}$ and $\lambda = \frac{\mu}{3}; \sigma = 2\lambda$, ensuring the generality of the path up to the critical limit. Remarkably, this investigation revealed thermodynamic-like features in a system with no obvious or traditional parallels. This achievement not only expands

our understanding of such unique systems, but also demonstrates their receptivity to the principles of critical phenomena theory.

In fact, our effort to compute critical exponents transcends the simple search for numerical precision, but rather serves as a test of the applicability of the theory of critical phenomena to the RPS model. This work confirms the consistency of the model with the theory, demonstrating its self-similarity near the critical point and the homogeneity of its correlation functions. Although our results pave the way for a deeper mathematical understanding of the RPS model in the context of critical phenomena, they also invite further exploration. It is possible to improve the understanding of the scaling laws found in the RPS model with the renormalization group theory approach [4]. As far as we know, this is the first study to investigate the deeper mathematical and physical aspects of the RPS model with the application of critical phenomena theory.

Overall, this work extends the application of critical phenomena theory to the dynamics of biological systems, marking an interdisciplinary approach that bridges physics and biology. The results of the present work confirm that the RPS model is consistent with Critical Phenomena Theory, and demonstrate its self-similarity and the homogeneity of the correlation functions near the critical point. By establishing a relation between critical phenomena and biological dynamics, this work provides the basis for a more general application of these principles, offering perspectives on the evolutionary behavior of species and the laws that govern both biological and physical systems. These efforts enhance our comprehension of the system and suggest new approaches to exploring the connections between critical phenomena theory and various scientific disciplines.

6 Summary and Conclusion

Our research aimed to establish the connection between the theory of critical phenomena [2] and the dynamics of the RPS model [17, 18, 27]. This interdisciplinary approach is based on a theoretical framework that combines scaling laws, universality, and phase transitions with cyclic dominance patterns observed in RPS systems [2, 40, 58]. We performed a series of large scale numerical simulations in the vicinity of the RPS critical point and analyzed the results using critical phenomena theory with the purpose of elucidating the emergence of critical behavior within these systems [17, 18, 27].

The methodology employed in our investigation consisted in conducting numerical simulations under different parameter settings in order to analyze the system behavior as it approached the critical point. For this, we approached the critical point thought two different paths corresponding to the constraints $\sigma = \lambda = \frac{\mu}{2}$ and $\lambda = \frac{\mu}{3}; \sigma = 2\lambda$, in order to test the generality of the critical behavior. We inferred that regardless of the trajectory in parameter space, the critical behavior was the same, thereby validating the universality of the observed phenomena [27, 34].

We reproduced the dynamics of competitive interactions and the transition from biodiversity to uniformity as the system approached the critical region [7, 9, 11]. Our simulations confirm the balance between diversity and uniformity in competitive systems; different states of the system were observed, such as the formation of clusters, the emergence of complex spiral patterns, and the eventual occupation of the entire lattice by a single species.

The homogeneity of the correlation function of the RPS model, in real as well as in reciprocal space, was the main conclusion of our analysis. This fundamental property allowed the application of rescaling techniques that enabled for the first time the determination of the critical point as well as the critical exponents for the RPS model by minimizing the mean square error of the rescaled correlation function. This approach enabled the calculation of the critical value for the movement parameter μ_c, the critical exponents ν, γ and, indirectly, the value of η using hyperscaling relations (3.26). Our method has demonstrated the applicability of the theoretical framework of critical phenomena theory to the complex dynamics of biological systems, as illustrated by the simplicity of the RPS model [2, 58].

In conclusion, the application of critical phenomena theory to the RPS model demonstrated its potential for the study of its complex dynamics. Our exhaustive exploration of the parameter space, aimed at minimizing errors and confirming the accuracy of the scaling behavior, reinforced the consistency of our results. Our work has extended the

application of critical phenomena theory to biological dynamics modeled by the RPS model, offering new perspectives on the behavior of species interactions. As a future perspective in this field of research, we suggest the application of group renormalization theory [4, 56] to the RPS model. This approach can clarify the reasons for the homogeneity of the correlation functions, as well as determine to which universality classes each variation of the RPS model belongs.

Bibliography

[1] L. P. Kadanoff, "Scaling laws for ising models near t_c," *Physics Physique Fizika*, vol. 2, no. 6, p. 263, 1966.

[2] H. E. Stanley, *Introduction to Phase Transitions and Critical Phenomena*. Oxford, 1971.

[3] M. E. Fisher, "Correlation functions and the critical region of simple fluids," *Journal of Mathematical Physics*, vol. 5, no. 7, pp. 944–962, 1964.

[4] K. G. Wilson, "Renormalization group and strong interactions," *Physical Review D*, vol. 3, no. 8, p. 1818, 1971.

[5] M. E. Fisher, "The theory of equilibrium critical phenomena," *Reports on progress in physics*, vol. 30, no. 2, p. 615, 1967.

[6] N. Goldenfeld, *Lectures on phase transitions and the renormalization group*. CRC Press, 2018.

[7] G. Szabó and G. Fáth, "Evolutionary games on graphs," *Physics reports*, vol. 446, no. 4-6, pp. 97–216, 2007.

[8] A. R. Ives and S. R. Carpenter, "Stability and diversity of ecosystems," *science*, vol. 317, no. 5834, pp. 58–62, 2007.

[9] A. Szolnoki, M. Mobilia, L.-L. Jiang, B. Szczesny, A. M. Rucklidge, and M. Perc, "Cyclic dominance in evolutionary games: a review," *Journal of the Royal Society Interface*, vol. 11, no. 100, p. 20140735, 2014.

[10] M. Graceand and M. T. Hütt, "Regulation of spatiotemporal patterns by biological variability: General principles and applications to dictyostelium discoideum," *PLoS computational biology*, vol. 11, no. 11, p. e1004367, 2015.

[11] S. Shibasaki and M. Shimada, "Cyclic dominance emerges from the evolution of two inter-linked cooperative behaviours in the social amoeba," *Proceedings of the Royal Society B*, vol. 285, no. 1881, p. 20180905, 2018.

[12] H. J. Zhou, "The rock–paper–scissors game," *Contemporary Physics*, vol. 57, no. 2, pp. 151–163, 2016.

[13] A. Szolnoki, B. F. de Oliveira, and D. Bazeia, "Pattern formations driven by cyclic interactions: A brief review of recent developments," *Europhysics Letters*, vol. 131, no. 6, p. 68001, 2020.

[14] B. Xu, H.-J. Zhou, and Z. Wang, "Cycle frequency in standard rock–paper–scissors games: evidence from experimental economics," *Physica A: Statistical Mechanics and its Applications*, vol. 392, no. 20, pp. 4997–5005, 2013.

[15] D. Bazeia, B. F. de Oliveira, J. V. O. Silva, and A. Szolnoki, "Breaking unidirectional invasions jeopardizes biodiversity in spatial may-leonard systems," *Chaos, Solitons & Fractals*, vol. 141, p. 110356, 2020.

[16] M. Hoffman, S. Suetens, U. Gneezy, and M. A. Nowak, "An experimental investigation of evolutionary dynamics in the rock-paper-scissors game," *Scientific reports*, vol. 5, no. 1, p. 8817, 2015.

[17] P. P. Avelino, D. Bazeia, L. Losano, J. Menezes, and B. F. de Oliveira, "Junctions and spiral patterns in generalized rock-paper-scissors models," *Physical Review E*, vol. 86, no. 3, p. 036112, 2012.

[18] P. P. Avelino, D. Bazeia, L. Losano, J. Menezes, and B. F. de Oliveira, "Interfaces with internal structures in generalized rock-paper-scissors models," *Physical Review E*, vol. 89, no. 4, p. 042710, 2014.

[19] H. E. Stanley, "Scaling, universality, and renormalization: Three pillars of modern critical phenomena," *Reviews of modern physics*, vol. 71, no. 2, p. S358, 1999.

[20] T. Reichenbach, M. Mobilia, and E. Frey, "Coexistence versus extinction in the stochastic cyclic lotka-volterra model," *Physical Review E*, vol. 74, no. 5, p. 051907, 2006.

[21] R. M. May, "Biological populations with nonoverlapping generations: stable points, stable cycles, and chaos," *Science*, vol. 186, no. 4164, pp. 645–647, 1974.

[22] H. Hermann, *Synergetics: introduction and advanced topics*. Springer Science, 2004.

[23] A. V. Suarez and N. D. Tsutsui, "The value of museum collections for research and society," *BioScience*, vol. 54, no. 1, pp. 66–74, 2004.

[24] A. J. Lotka, "Undamped oscillations derived from the law of mass action," *Journal of the american chemical society*, vol. 42, no. 8, pp. 1595–1599, 1920.

[25] B. Sinervo and C. M. Lively, "The rock–paper–scissors game and the evolution of alternative male strategies," *Nature*, vol. 380, no. 6571, p. 240, 1996.

[26] B. Sinervo, D. B. Miles, W. A. Frankino, M. Klukowski, and D. F. DeNardo, "Testosterone, endurance, and darwinian fitness: natural and sexual selection on the physiological bases of alternative male behaviors in side-blotched lizards," *Hormones and Behavior*, vol. 38, no. 4, pp. 222–233, 2000.

[27] T. Reichenbach, M. Mobilia, and E. Frey, "Mobility promotes and jeopardizes biodiversity in rock–paper–scissors games," *Nature*, vol. 448, no. 7157, p. 1046, 2007.

[28] D. Bazeia, M. Bongestab, B. F. de Oliveira, and A. Szolnoki, "Effects of a pestilent species on the stability of cyclically dominant species," *Chaos, Solitons & Fractals*, vol. 151, p. 111255, 2021.

[29] P. Hohenberg and B. I. Halperin, "Theory of dynamic critical phenomena," *Reviews of Modern Physics*, vol. 49, no. 3, p. 435, 1977.

[30] L.-L. Jiang, W.-X. Wang, and B.-H. Wang, "Pattern formation in spatial games," *Physics Procedia*, vol. 3, no. 5, pp. 1933–1939, 2010.

[31] B. F. de Oliveira, M. V. de Moraes, D. Bazeia, and A. Szolnoki, "Mobility driven coexistence of living organisms," *Physica A: Statistical Mechanics and its Applications*, vol. 572, p. 125854, 2021.

[32] D. Bazeia, M. J. B. Ferreira, B. F. de Oliveira, and A. Szolnoki, "Environment driven oscillation in an off-lattice may–leonard model," *Scientific Reports*, vol. 11, no. 1, p. 12512, 2021.

[33] D. Bazeia, M. Bongestab, and B. F. de Oliveira, "Influence of the neighborhood on cyclic models of biodiversity," *Physica A: Statistical Mechanics and its Applications*, vol. 587, p. 126547, 2022.

[34] L.-L. Jiang, T. Zhou, M. Perc, and B.-H. Wang, "Effects of competition on pattern formation in the rock-paper-scissors game," *Physical Review E*, vol. 84, no. 2, p. 021912, 2011.

[35] R. Folk and G. Moser, "Critical dynamics: a field-theoretical approach," *Journal of Physics A: Mathematical and General*, vol. 39, no. 24, p. R207, 2006.

[36] R. Souza, A. Pelster, and F. E. A. dos Santos, "Green's function approach to the bose–hubbard model with disorder," *New Journal of Physics*, vol. 23, no. 8, p. 083007, 2021.

[37] R. Souza, A. Pelster, and F. E. A. dos Santos, "Emergence of damped-localized excitations of the mott state due to disorder," *New Journal of Physics*, vol. 25, no. 6, p. 063015, 2023.

[38] M. Scheffer, S. R. Carpenter, T. M. Lenton, J. Bascompte, W. Brock, V. Dakos, J. Van de Koppel, I. A. Van de Leemput, S. A. Levin, E. H. Van Nes, *et al.*, "Anticipating critical transitions," *science*, vol. 338, no. 6105, pp. 344–348, 2012.

[39] V. Dakos, S. R. Carpenter, W. A. Brock, A. M. Ellison, V. Guttal, A. R. Ives, S. Kéfi, V. Livina, D. A. Seekell, E. H. van Nes, *et al.*, "Methods for detecting early warnings of critical transitions in time series illustrated using simulated ecological data," *PloS one*, vol. 7, no. 7, p. e41010, 2012.

[40] F. E. A. dos Santos, *Ginzburg-Landau theory for bosonic gases in optical lattices*. PhD thesis, Freie Universität Berlin, 2011.

[41] S. H. Strogatz, *Nonlinear dynamics and chaos with student solutions manual: With applications to physics, biology, chemistry, and engineering*. CRC press, 2018.

[42] M. Batty, "Fractals-geometry between dimensions," *New Scientist*, vol. 105, 1985.

[43] E. Mäkinen, "A survey on binary tree codings," *The Computer Journal*, vol. 34, no. 5, pp. 438–443, 1991.

[44] M. F. Barnsley, *Fractals everywhere*. Academic press, 1988.

[45] M. Thiriet, *Anatomy and physiology of the circulatory and ventilatory systems*, vol. 6. Springer, 2014.

[46] B. B. Mandelbrot and B. B. Mandelbrot, *The fractal geometry of nature*, vol. 1. WH freeman New York, 1982.

[47] E. Azpeitia, G. Tichtinsky, M. Le Masson, A. Serrano-Mislata, J. Lucas, V. Gregis, C. Gimenez, N. Prunet, E. Farcot, M. M. Kater, *et al.*, "Cauliflower fractal forms arise from perturbations of floral gene networks," *Science*, vol. 373, no. 6551, pp. 192–197, 2021.

[48] J. D. Pelletier and D. L. Turcotte, "Shapes of river networks and leaves: are they statistically similar?," *Philosophical Transactions of the Royal Society of London. Series B: Biological Sciences*, vol. 355, no. 1394, pp. 307–311, 2000.

[49] J. T. Perron, P. W. Richardson, K. L. Ferrier, and M. Lapôtre, "The root of branching river networks," *Nature*, vol. 492, no. 7427, pp. 100–103, 2012.

[50] B. Mandelbrot, "How long is the coast of britain? statistical self-similarity and fractional dimension," *science*, vol. 156, no. 3775, pp. 636–638, 1967.

[51] J. Nelson, "Branch growth and sidebranching in snow crystals," *Crystal growth & design*, vol. 5, no. 4, pp. 1509–1525, 2005.

[52] M. Frame and A. Urry, *Fractal worlds: Grown, built, and imagined*. Yale University Press, 2016.

[53] L. Moyano, J. De Souza, and S. D. Queirós, "Multi-fractal structure of traded volume in financial markets," *Physica A: Statistical Mechanics and its Applications*, vol. 371, no. 1, pp. 118–121, 2006.

[54] L. Kristoufek, "Fractal markets hypothesis and the global financial crisis: Scaling, investment horizons and liquidity," *Advances in Complex Systems*, vol. 15, no. 06, p. 1250065, 2012.

[55] K. Huang, *Statistical mechanics*. John Wiley and Sons, 1987.

[56] A. N. Vasil'ev, *The field theoretic renormalization group in critical behavior theory and stochastic dynamics*. Chapman and Hall/CRC, 2004.

[57] H. Kleinert and V. Schulte-Frohlinde, *Critical Properties of ϕ^4 - theories*. World Scientific, 2001.

[58] P. D. Beale, *Statistical Mechanics*. Butterworth-Heinemann, 1996.

[59] G. Chapline Jr, "Theory of the superfluid transition in liquid helium," *Physical Review A*, vol. 3, no. 5, p. 1671, 1971.

[60] A. Cidrim, A. White, A. Allen, V. S. Bagnato, and C. Barenghi, "Vinen turbulence via the decay of multicharged vortices in trapped atomic bose-einstein condensates," *Physical Review A*, vol. 96, no. 2, p. 023617, 2017.

[61] M. Raju, A. Van Duin, and M. Ihme, "Phase transitions of ordered ice in graphene nanocapillaries and carbon nanotubes," *Scientific reports*, vol. 8, no. 1, p. 3851, 2018.

[62] G. Shirane, "Neutron scattering studies of structural phase transitions at brookhaven," *Reviews of Modern Physics*, vol. 46, no. 3, p. 437, 1974.

[63] M. Lerch, H. Boysen, R. Neder, F. Frey, and W. Laqua, "Neutron scattering investigation of the high temperature phase transition in nitio3," *Journal of Physics and Chemistry of Solids*, vol. 53, no. 9, pp. 1153–1156, 1992.

[64] M. Continentino, "Quantum scaling in many-body systems," *Physics reports*, vol. 239, no. 3, pp. 179–213, 1994.

[65] M. Zare and P. Grigolini, "Criticality and avalanches in neural networks," *Chaos, Solitons & Fractals*, vol. 55, pp. 80–94, 2013.

[66] J. L. McCauley, *Dynamics of markets: The new financial economics*. Cambridge University Press, 2009.

[67] B. I. Halperin and P. C. Hohenberg, "Scaling laws for dynamic critical phenomena," *Physical Review*, vol. 177, no. 2, p. 952, 1969.

[68] L. D. Landau and E. M. Lifshitz, *Course of theoretical physics*. Pergamon Press Ltd, 1980.

[69] M. A. G. dos Santos Filho and F. E. A. dos Santos, "Incompressible energy spectrum from wave turbulence," *Physica D: Nonlinear Phenomena*, vol. 440, p. 133479, 2022.

[70] S. Kirkpatrick, C. D. Gelatt Jr, and M. P. Vecchi, "Optimization by simulated annealing," *science*, vol. 220, no. 4598, pp. 671–680, 1983.

[71] P. Weiss, "L'hypothèse du champ moléculaire et la propriété ferromagnétique," *J. Phys. Theor. Appl.*, vol. 6, no. 1, pp. 661–690, 1907.

[72] L. Onsager, "Crystal statistics. i. a two-dimensional model with an order-disorder transition," *Physical Review*, vol. 65, no. 3-4, p. 117, 1944.

[73] B. Widom, "Equation of state in the neighborhood of the critical point," *The Journal of Chemical Physics*, vol. 43, no. 11, pp. 3898–3905, 1965.